Since January 2020 Elsevier has created a COVID-19 resource centre with free information in English and Mandarin on the novel coronavirus COVID-19. The COVID-19 resource centre is hosted on Elsevier Connect, the company's public news and information website.

Virus Research 202 (2015) 12–32

Contents lists available at ScienceDirect

Virus Research

journal homepage: www.elsevier.com/locate/virusres

What we know but do not understand about nidovirus helicases

Kathleen C. Lehmann[a], Eric J. Snijder[a], Clara C. Posthuma[a], Alexander E. Gorbalenya[a,b,*]

[a] Department of Medical Microbiology, Leiden University Medical Center, Leiden, The Netherlands
[b] Faculty of Bioengineering and Bioinformatics, Lomonosov Moscow State University, Russia

ARTICLE INFO

Article history:
Available online 8 December 2014

Keywords:
Antiviral drugs
Coronavirus
Discontinuous RNA synthesis
Post-transcriptional quality control
Viral replication
Superfamily 1 helicase

ABSTRACT

Helicases are versatile NTP-dependent motor proteins of monophyletic origin that are found in all kingdoms of life. Their functions range from nucleic acid duplex unwinding to protein displacement and double-strand translocation. This explains their participation in virtually every metabolic process that involves nucleic acids, including DNA replication, recombination and repair, transcription, translation, as well as RNA processing. Helicases are encoded by all plant and animal viruses with a positive-sense RNA genome that is larger than 7 kb, indicating a link to genome size evolution in this virus class. Viral helicases belong to three out of the six currently recognized superfamilies, SF1, SF2, and SF3. Despite being omnipresent, highly conserved and essential, only a few viral helicases, mostly from SF2, have been studied extensively. In general, their specific roles in the viral replication cycle remain poorly understood at present. The SF1 helicase protein of viruses classified in the order *Nidovirales* is encoded in replicase open reading frame 1b (ORF1b), which is translated to give rise to a large polyprotein following a ribosomal frameshift from the upstream ORF1a. Proteolytic processing of the replicase polyprotein yields a dozen or so mature proteins, one of which includes a helicase. Its hallmark is the presence of an N-terminal multinuclear zinc-binding domain, the nidoviral genetic marker and one of the most conserved domains across members of the order. This review summarizes biochemical, structural, and genetic data, including drug development studies, obtained using helicases originating from several mammalian nidoviruses, along with the results of the genomics characterization of a much larger number of (putative) helicases of vertebrate and invertebrate nidoviruses. In the context of our knowledge of related helicases of cellular and viral origin, it discusses the implications of these results for the protein's emerging critical function(s) in nidovirus evolution, genome replication and expression, virion biogenesis, and possibly also post-transcriptional processing of viral RNAs. Using our accumulated knowledge and highlighting gaps in our data, concepts and approaches, it concludes with a perspective on future research aimed at elucidating the role of helicases in the nidovirus replication cycle.

1. Helicases: conserved but versatile players in biological processes utilizing nucleic acids in viruses and hosts

Cellular life forms in all kingdoms, as well as positive-strand RNA (+RNA) viruses with a genome larger than 7 kb and a number of DNA viruses, encode (predicted) helicases on which they depend in various ways (Fairman-Williams et al., 2010; Gorbalenya and Koonin, 1989). Helicases are widely recognized for their capability to resolve base pairs in nucleic acid duplexes in an NTP- and metal-dependent manner (Fig. 1A and D). Additionally, some helicases were shown to displace proteins present in polynucleotide–protein complexes (Fig. 1B) (Singleton et al., 2007) and to translocate along double-stranded DNA or RNA without unwinding it (Fig. 1C) (Singleton et al. 2007; Jankowsky and Fairman 2007). Besides replication, their unwinding activity may be utilized in many other processes including, but not limited to, DNA repair, transcription, RNA maturation and splicing, and translation. Thus, it is not surprising that as much as 1% of all prokaryotic and eukaryotic genes were estimated to encode helicases (Gorbalenya and Koonin, 1993).

1.1. Helicase classification and domain organization

Helicases are classified into six evolutionary compact and interrelated superfamilies (SFs 1–6) which were established using statistically significant sequence similarity, corroborated and extended by subsequent structural analyses of selected members (Gorbalenya and Koonin, 1993; Singleton et al., 2007). Among the SF members classified are relatively few characterized helicases and

* Corresponding author at: Department of Medical Microbiology, Leiden University Medical Center, P.O. Box 9600, 2300-RC Leiden, The Netherlands.
Tel.: +31 71 526 1652; fax: +31 71 526 6761.
E-mail address: a.e.gorbalenya@lumc.nl (A.E. Gorbalenya).

http://dx.doi.org/10.1016/j.virusres.2014.12.001
0168-1702/

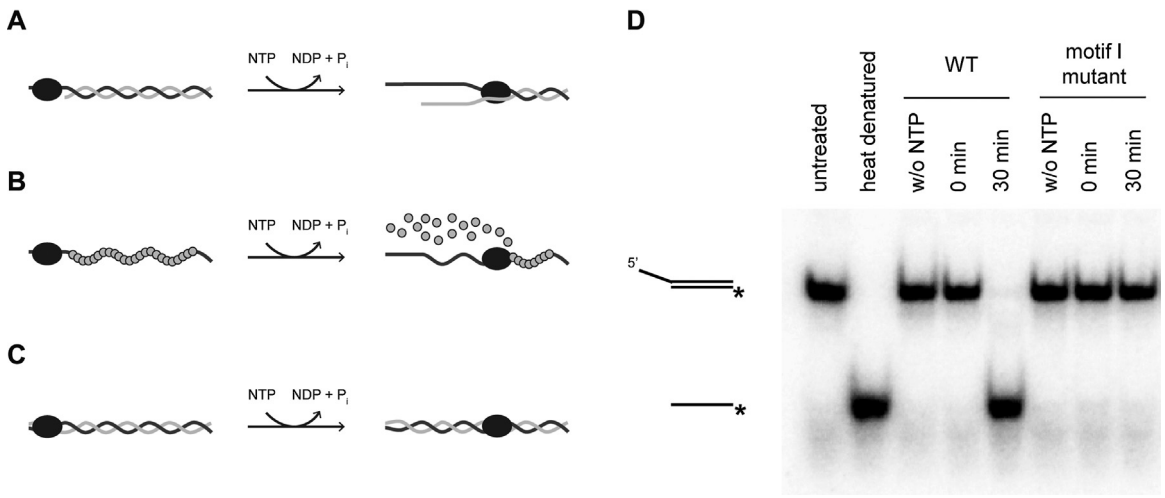

Fig. 1. Schematic representation of NTP-dependent helicase activities. (A) Unwinding of a nucleic acid duplex. (B) Displacement of protein bound to nucleic acid. (C) Translocation along a double-stranded nucleic acid without unwinding. (D) Typical result of a biochemical nucleic acid unwinding assay. Shown is the helicase activity of equine arteritis virus (EAV) nsp10 and a corresponding active site mutant carrying a Lys-164 to Gln substitution in motif I. The asterisk marks the position of the radioactive label.

Panel D is adapted from Deng et al. (2014).

numerous related proteins, whose number has steadily increased along with genomics projects. The helicase SFs are distinguished by characteristic conserved sequences (motifs) that are often used to identify new members. Helicases of the two larger superfamilies SF1 and SF2 are characterized by their monomeric or dimeric state and the presence of up to twelve conserved sequence motifs involved in NTP and nucleic acid binding and the coordination thereof (Fairman-Williams et al., 2010; Gorbalenya et al., 1989b; Singleton et al., 2007). In contrast, SFs 3–6 require the formation of hexamers or dodecamers in order to be active and contain just three to four signature motifs. Only some of these motifs are specific to a particular superfamily, while others may be conserved in a more or less diverse group of proteins. For instance, motifs I and II (or the Walker A and B boxes, respectively (Walker et al., 1982)), are common to all helicase SFs and are also conserved in many NTPases that lack helicase activity, attesting to the fact that helicases form an evolutionary lineage within a very diverse class of NTP-utilizing enzymes. All motifs are embedded in a catalytic core. In SF1 and SF2, it is formed by two RecA-like domains, designated 1A and 2A, that emerged by duplication and extensive divergence (Subramanya et al., 1996; Korolev et al., 1997; Kim et al., 1998). In contrast, members of SFs 3–6 employ a helicase core composed of a single RecA-like domain. It is this helicase core which essentially allows the conversion of chemical energy stored in NTP phosphodiester bonds to mechanical energy that fuels the directional movement of the protein along a nucleic acid strand. SF1 and SF2 members typically include additional domains that may be located upstream and/or downstream of 1A and 2A, or inserted within those domains. In some helicase proteins, the size of these accessory domains exceeds that of the actual helicase core domains. Such insertions are thought to govern specific protein functions, including helicase activity *per se*, by engaging in protein–protein and protein–nucleic acid interactions or through additional enzymatic activities. This modular design contributes importantly to the versatility of this enzyme group and serves to achieve specificity (Fairman-Williams et al., 2010; Singleton et al., 2007; Singleton and Wigley, 2002).

1.2. SF1 helicases

The SF1 helicases, which are the focus of this review, have been further subdivided into three distinct families using structural and biochemical considerations (Singleton et al., 2007) (Table 1). Each family was named after its most prominent members of the moment: UvrD/Rep, Pif1-like, and Upf1-like. The most striking difference between these families is the direction of translocation along their nucleic acid substrate. Relative to the single strand with which they associate, members of the first family traverse their substrate in the 3′–5′ direction (type A), whereas members of the other two families are moving from 5′ to 3′ (type B). A second distinguishing feature is the nucleic acid substrate preference, which is thought to be exclusive for DNA for the UvrD/Rep and Pif1-like families. In contrast, the Upf1-like family comprises members that may unwind either DNA or RNA, and in some cases both without a clear preference. As mentioned, the number of helicases identified through comparative genomics (so-called putative helicases) far exceeds the number of proven and structurally characterized helicases. Consequently, it remains uncertain whether the above regularities faithfully reflect a different mode of nucleic acid binding in these families (Fairman-Williams et al., 2010) or are due to a sampling bias of the characterized helicases.

1.3. SF1 helicases of RNA viruses

Viral helicases belong to one of three superfamilies, SF1 (*e.g.* alphavirus-like viruses, nidoviruses, herpesviruses), SF2 (*e.g.* flaviviruses, herpesviruses), or SF3 (*e.g.* picornavirus-like viruses), with their role in the viral replicative cycle remaining largely unknown for any RNA virus (Gorbalenya et al., 1989a; Gorbalenya and Koonin, 1993; Kadare and Haenni, 1997). Given the apparent correlation between genome size and the presence of a helicase (Gorbalenya and Koonin, 1989), it was speculated that these enzymes could either reduce the nucleotide misincorporation (Koonin, 1991) or assist RdRp in unwinding of long double-stranded regions (Gorbalenya et al., 2006) during replication of +RNA viral genomes above a certain size threshold. Thus, expression of a helicase protein may be particularly important for viruses of the order *Nidovirales*, comprising the families *Arteriviridae*, *Coronaviridae*, *Mesoniviridae*, and *Roniviridae*, which are characterized by having large to very large +RNA genomes (13–34 kb) (Lauber et al., 2013; Stenglein et al., 2014; de Groot et al., 2012).

In this review, we will summarize the state of the art of our knowledge and recent advances in our understanding of these nidovirus enzymes. In particular, we will emphasize

Table 1
Biochemical properties of selected SF1 helicases.

Structure-based classification	Nucleotide substrate				Nucleic acid substrate		Unwinding polarity
	ATP	Other NTPs[a]	dATP	Other dNTPs[a]	DNA	RNA	
UvrD/Rep family							
UvrD[b]	+	–	+	–	+	n.d.	3′–5′
Rep[c]	+	–	+	–	+	n.d.	3′–5′
PcrA[d]	+	+	+	+	+	n.d.	3′–5′
Pif1-like family							
Pif1[e]	+	+	+	+	+	n.d.	5′–3′
RecD[f]	+	+	n.d.	n.d.	+	n.d.	5′–3′
Dda[g]	+	–	+	–	+	n.d.	5′–3′
Upf1-like family							
Upf1[h]	+	–	+	–	+	+	5′–3′
Nidovirus helicases[i]	+	+	+	+	+	+	5′–3′
Alphavirus nsP2[j,k]	+	+	+	+	–	+	5′–3′
Hepevirus Hel[k,l]	+	+	+	+	–	+	5′–3′
Alphatetravirus Hel[k,m]	+	+	+	+	–	+	5′–3′

n.d., not done.
[a] Considered negative if activity <10% of ATPase activity.
[b] Hickson et al. (1983), Matson (1986) and Matson and George (1987).
[c] Arai et al. (1981), Wong et al. (1996) and Yarranton and Gefter (1979).
[d] Bird et al. (1998).
[e] Lahaye et al. (1991) and Lahaye et al. (1993).
[f] Chen et al. (1997).
[g] Hacker and Alberts (1992) and Jongeneel et al. (1984).
[h] Bhattacharya et al. (2000) and Czaplinski et al. (1995).
[i] Adedeji et al. (2012a), Bautista et al. (2002), Ivanov and Ziebuhr (2004), Seybert et al. (2000a,b) and Tanner et al. (2003).
[j] Das et al. (2014), Karpe et al. (2011), Karpe and Lole (2010a) and Xiang et al. (2012).
[k] Based on biochemical properties and a high structural similarity of domains 1A and 2A of tomato mosaic virus Hel to those found in Upf1 we propose to classify the related alphavirus nsP2, and hepevirus and alphatetravirus orthologs with proven helicase activity in the Upf1-like family.
[l] Karpe and Lole (2010a).
[m] Wang et al. (2012).

similarities and differences between nidovirus helicases and other viral and non-viral SF1 helicases, and their implications for helicase functions in the nidovirus replication cycle. We will start with a summary of our understanding of the structural organization and enzymatic activities of SF1 helicases which is based on the analysis of few cellular enzymes. In our comparative analysis we will frequently refer to SF1 helicases of the alphavirus-like supergroup, the only other large group of +RNA viruses that uniformly encodes a SF1 helicase (Gorbalenya et al., 1988; Nishikiori et al., 2012). Among this supergroup, which includes a dozen animal and plant virus families with +RNA genomes in the size range of 7–20 kb, the helicases of the animal alphaviruses Semliki Forest virus (SFV) and chikungunya virus (CHIKV), the hepevirus hepatitis E virus (HEV), the alphatetravirus dendrolimus punctatus tetravirus as well as the plant tobamovirus tomato mosaic virus (ToMV) have been biochemically or structurally characterized to some extent (Das et al., 2014; Gomez de Cedron et al., 1999; Karpe et al., 2011; Karpe and Lole, 2010a,b; Nishikiori et al., 2012; Wang et al., 2012). To limit the scope of this review, comparisons are restricted to data on these proteins, while the large body of literature on the genetics of helicase mutants of alphavirus-like plant viruses (*e.g.* see Wang et al., 2005) is not discussed.

2. The structural basis for helicase translocation, directionality, and unwinding

When characterizing helicases enzymatically and structurally, some of the major questions asked address the type of substrate used, the direction of movement, rate and processivity, the coupling of helicase properties to specific biological functions, and the regulation of the enzymes' activities. In this section, we will briefly summarize our understanding of mechanisms of SF1 helicase unwinding and directional movement along a nucleic acid. Helicases may unwind polynucleotides that are either fully or partially double-stranded, including DNA/DNA, DNA/RNA or RNA/RNA duplexes (Fig. 1A). Since they provide the initiation sites for unwinding, single-stranded overhangs of these substrates, if present, may provide specificity to the enzyme–substrate interaction through their sequence, size, or structure, or a combination thereof. SF1 and SF2 include helicases with diverse biochemical properties, including directionality and substrate preference; these properties, *e.g.* 5′–3′ directionality of movement, may thus have evolved more than once (convergent evolution). In comparative terms, they are less conserved than the sequence motifs that define a superfamily. Consequently, understanding the underlying selection pressure that drives the conservation of these motifs may provide a separate and vital insight into helicase function.

2.1. Functions of conserved sequence motifs

As outlined above, despite sequence conservation and similar fold of the core domains, a fundamental difference must exist in the way in which helicase proteins of SF1A and SF1B interact with their nucleic acid substrate in order to achieve translocation, and thus unwinding, with a defined polarity. To shed light on the mechanistic basis of this difference, we first need to understand the general molecular mechanism by which directional movement is generated driven by the energy originating from NTP hydrolysis. As one would expect, the elements involved in this essential NTPase activity are generally conserved among SF1 helicases (Fig. 2A and B) and (in part) beyond, reflecting considerable evolutionary constraints (Fairman-Williams et al., 2010). The most notable of these are motifs I and II, which harbor key residues necessary for the direct interaction with the NTP:Mg^{2+} and NDP:Mg^{2+} complexes. Furthermore, motif II contains a conserved glutamate thought to act as catalytic base during hydrolysis by accepting a proton from the water molecule that subsequently attacks the NTP (Subramanya et al., 1996). Other motifs vary in respect to sequence conservation

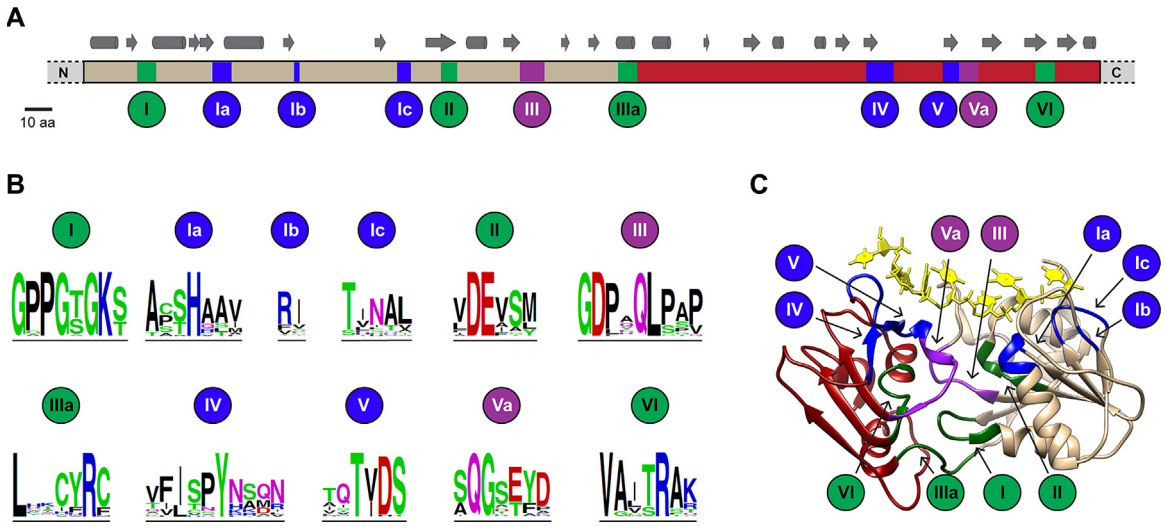

Fig. 2. Conservation, structure, and function of the SF1 helicase core domains 1A (light-brown) and 2A (red). Shown are properties of nidovirus helicases, which may deviate from other SF1 helicases. (A) Relative positions of motifs and secondary structure elements of a consensus nidovirus helicase. Secondary structures were predicted by Jpred (Cole et al., 2008) using a multiple sequence alignment of 31 representative nidoviruses that was assisted by tools in the Viralis software platform (Gorbalenya et al., 2010). Motifs as defined in Fairman-Williams et al. (2010) are colored according to their predominant biochemical function. Green, NTP binding and hydrolysis; blue, nucleic acid binding; purple, coupling between NTP and nucleic acid binding sites. (B) Sequence conservation of helicase signature motifs of representative nidoviruses depicted using WebLogo (Crooks et al., 2004). Motifs Q (LNxxQ) and Vb (xxxxVR) are absent in nidoviruses. (C) Position of sequence motifs in the tertiary structure of the EAV nsp10 helicase core with the modelled single-stranded nucleic acid shown in yellow (PDB accession number 4N0O).

and diversity of helicases with whom they are associated. Motifs Ia, III, IV, V, Va, and VI are found in SF1 and SF2. Of these, motifs III, IV, V, Va, and VI are most conserved, with motifs III and VI having the most distinctive signatures of each helicase superfamily. Additionally, motif IIIa is found exclusively in SF1 helicases, while motifs Q, Ib, Ic and Vb may be specific to different subsets of SF1 helicases. For instance, motifs Q and Vb are apparently absent in nidovirus helicases (Fig. 2).

Additional nucleotide-binding residues reside in motifs Q, IIIa, and VI. The first two of these seem to be specifically important for the recognition of ATP. Thus, it is not surprising that the Q motif and a conserved tyrosine in motif IIIa that provides stacking interactions with the adenine base may be lacking in helicases without nucleotide specificity, such as that of ToMV (Nishikiori et al., 2012). Moreover, a highly conserved arginine residue in motif VI, termed "arginine finger", specifically interacts with the γ-phosphate of the incoming NTP. Relative to motifs I, II, and Q this residue is located on the opposite side of the NTP-binding cleft formed by domains 1A and 2A (Fig. 2C). This position enables it to fulfill a critical function in opening and closing of the cleft in response to NTP binding and hydrolysis, which triggers a conformational shift at the NTP binding site that is translated into a rotation of domain 2A toward 1A (Cheng et al., 2007; Saikrishnan et al., 2009; Velankar et al., 1999). Although this domain movement is a common feature, the exact mechanism and kinetics of hydrolysis and product release may differ between helicases, possibly in response to specific physiological roles (Toseland et al., 2009).

To translate the rotation into movement along a nucleic acid track, the majority of the remaining (partially) conserved motifs is primarily devoted to nucleic acid binding (motifs Ia-c, IV, IVa, V, and Vb). These motifs are located exclusively on the opposite face of the helicase core relative to the nucleotide binding site, resulting in a nucleic acid-binding channel involving both core domains on the one side and additional protein-specific domains on the other. Interestingly, while SF1A helicases are thought to establish contacts mainly *via* base stacking, members of SF1B seem to bind predominantly to the phosphate-sugar backbone. This would suggest that SF1A helicases are strongly inhibited by base lesions, while SF1B members would not tolerate backbone modifications (Saikrishnan et al., 2009). Moreover, the crystal structure of the DNA-specific Pif1-like helicase RecD2 revealed a C3′ endo conformation of the sugar backbone of a bound DNA. As this conformation appeared to be heavily stabilized by amino acid side chain interactions, it was speculated that this binding mode may be the basis for discrimination against RNA, whose 2′-OH would prevent establishing these interactions (Saikrishnan et al., 2009). In further support of this hypothesis, similar interactions are conserved in other DNA helicases like Rep, PcrA, and RecB, while they cannot be found in Upf1 which can utilize both DNA and RNA (Cheng et al., 2007; Korolev et al., 1997; Singleton et al., 2004; Velankar et al., 1999). Finally, motifs III and Va contact both NTP and nucleic acid binding sites to promote coupling of the binding processes (Fairman-Williams et al., 2010). Thus, it is not surprising to observe that NTP hydrolysis is inhibited if helicase translocation is prevented (Lohman and Bjornson, 1996; Maine and Kodadek, 1994).

2.2. *General models of translocation: how the energy of NTP-hydrolysis is converted into directional movement*

In an effort to explain the sequence of events that enables the conversion of the NTP hydrolysis-induced domain rotation into a directional movement, two hypotheses have been brought forward: the Brownian motor hypothesis (Levin et al., 2005) and the 'backbone stepping motor' model (Wong and Lohman, 1992; Yarranton and Gefter, 1979). The former, based on the observation that the SF2 helicase (NS3) of Hepatitis C virus (HCV) has lower nucleic acid affinity in the NTP-bound state than in the free state, explains the directional translocation on the basis of Brownian motion and a 'power stroke' caused by NTP-hydrolysis. Furthermore, it assumes an asymmetric sawtooth-shaped energy profile for helicase binding to nucleic acids over the length of the single strand. In the absence of NTP, the enzyme would bind strongly to the nucleic acid and thus be incapable of any movement, a state characterized by a local energy minimum. Conversely, once NTP binds, the enzyme's affinity for nucleic acid decreases, which triggers either the dissociation of the protein or its random movement covering a certain number of bases. During this stage, existing energy barriers may be fully or partially overcome. When the NTP

is hydrolyzed and the enzyme's affinity for its nucleic acid substrate is restored, the protein may either fall into a neighboring local energy minimum or return to the original one. However, since the energy profile is assumed to be asymmetric, *i.e.* a shorter, steeper barrier exists on one side of the helicase, the enzyme would be more likely to overcome a local energy maximum in one direction than the other, resulting in a net forward motion. Although this model presents a simple thermodynamic perspective on protein translocation, it has remained unclear which protein or nucleic acid properties would play a role in creating the required asymmetric energy profile (Levin et al., 2005).

Two main variants have been proposed for the 'backbone stepping motor' model, which also relies on sequential NTP-dependent affinity changes: the 'active rolling' model by Wong and Lohman (1992), and the 'inchworm' model, originally from Yarranton and Gefter (1979) and extended by Velankar et al. (1999). Although these models are quite similar, there is one decisive difference: the proposed number of binding sites per enzyme. The former model proposes the existence of a single nucleic acid binding site per helicase subunit, which allows binding to either single- or double-stranded nucleic acids. Thus, in order to engage simultaneously with the transition region between duplex and single strand, the so-called "fork", at least a functional enzyme dimer is required. Upon NTP hydrolysis, the individual subunits of this dimer are then assumed to "roll" over each other, resulting in a constant replacement of the leading molecule. This model thus implies a step size, defined as the distance that a helicase moves forward during a single catalytic cycle, at least equaling the size of each individual binding site. In contrast, the inchworm mechanism postulates the existence of two binding sites within the same helicase subunit, allowing the protein to "slide" along a nucleic acid. Therefore, neither the oligomerization state nor the unwinding step size would be subject to any constraints.

In support of the latter model, all helicase crystal structures currently available show a monomeric protein, even in those cases where the co-crystallized nucleic acid would have allowed binding of a second subunit (Velankar et al., 1999). Furthermore, biochemical data demonstrating step sizes of one base pair exist for several helicases (Dillingham et al., 2000; Tomko et al., 2007), which is difficult to reconcile with the active rolling model unless it would include a backward motion at some point in the reaction cycle. As this would imply a deliberately low efficiency of unwinding, this is unlikely to be the case. An additional conflict with the active rolling model derives from studies with PcrA, which was not found to dimerize yet displayed a higher affinity for substrates comprised of single- and double-stranded regions than for those containing exclusively either of these states (Bird et al., 1998). This essentially argues against the strict temporal separation of single- and double-strand binding. It should be noted that the kinetic data derived from studies with Rep and UvrD that served as the basis for the rolling model are consistent with the inchworm mechanism as well.

2.3. The structural basis for directionality

Given the large body of experimental data supporting it, the inchworm model is now widely accepted. The model (Fig. 3, top panel) based on the SF1A helicase PcrA proposes two intermediate steps that are characterized by different affinities for a DNA substrate, a feature controlled by the binding and hydrolysis of NTPs. Initially, the helicase protein binds to a single strand in the 3′–5′ orientation, utilizing all binding pockets present in the 1A and 2A domains. Of special importance is a phenylalanine in motif Ia, located in domain 1A and conserved in the UvrD/Rep subfamily of SF1 (Dillingham et al., 2001) but replaced by different residues in nidoviruses (2nd residue in motif Ia of Fig. 2B). It fulfills the role of gatekeeper for the second of three base acceptor pockets within this domain (named A to C in the 3′–5′ direction) (Fig. 3, top panel). Once NTP binds to the NTP binding site, inducing the closure of the binding cleft, the conformational change is relayed to this residue and causes the displacement of the base residing in pocket B into pocket A. At this point, only two of three binding sites of 1A are occupied and thus the overall affinity for DNA is reduced. Since domain 2A retains its grip on the DNA and both core domains rotate toward each other, 1A is pulled along the substrate in 3′–5′ direction. Subsequently, NTP hydrolysis triggers the re-opening of pocket B and allows the next base to enter. Ultimately, binding of a base to the vacant binding pocket in 1A initiates a cascade of base movements and re-establishes the initial strong binding of 1A. In conjunction with the re-opening of the NTP binding cleft, 2A is now pushed away from 1A, completing the translocation step in 3′–5′ direction (Velankar et al., 1999).

In order to change the direction of translocation to fulfill alternative cellular functions, two variations of this mechanism would be conceivable: the helicase could bind to nucleic acids in the opposite orientation or the order of binding events could be reversed. Using the SF1B prototype helicase RecD2, Saikrishnan et al. (2009) demonstrated that the latter is true for this protein. Although the overall binding site and its location resemble those of SF1A helicases, subtle differences in what seems to be an otherwise remarkably similar mechanism became apparent (Fig. 3, bottom panel). In particular, it is noteworthy that the conserved phenylalanine of motif Ia is not present in SF1B helicases but is, as in SF2 helicases, often replaced by a conserved proline (Saikrishnan et al., 2008). While this replacement results in the loss of the gatekeeping function for this residue, the pocket mentioned above still plays a major role during translocation. Before NTP binding, it is occupied by a base, which has to flip out of the stacked conformation with its neighboring bases in order to bind. Together with several other contacts with the DNA backbone, this leads to a firm interaction between domain 1A and the single strand. As soon as the NTP is bound and cleft closure induced, the conformational change of the NTP-binding cleft translates directly into several alterations and concomitant strengthening of the interaction network of 2A. However, as a number of contacts are made with the downstream base compared to the NTP-free state, it seems that, in contrast to the mechanism for 3′–5′ translocation, 2A becomes the dominant binding domain only after the domain movement has been completed. In parallel, the base in the motif Ia pocket moves back into a stacked conformation, releasing the mechanical block on 1A movement. This conformational switch may be facilitated by relaxation of the DNA as 2A moves toward 1A. Finally, as the NTP is hydrolyzed, the binding cleft re-opens and pushes 1A toward the 3′ end, concluding the 5′–3′ translocation by one base.

Although both models offer a compelling mechanism for the directional movement of helicases, it needs to be stressed that both are based on the analysis of just two crystal structures, one in the absence and one in the presence of NTPs, which were obtained for very different helicases representing SF1A and SF1B, respectively, Thus it is possible that, when more structures become available, additional transition states might be identified in the catalytic cycle, possibly leading to revision or elaboration of the proposed mechanisms. Also, these mechanisms must be correlated with evolutionary conservation of key residues, which will require insights that may not be deducible from the helicase family classification (SF1A and SF1B) founded on structural and biochemical considerations.

2.4. Mechanisms of strand separation: do helicases play an active or passive role?

As the translocation of a helicase strictly occurs along a single strand, the energy spent on this process could, in principle, also

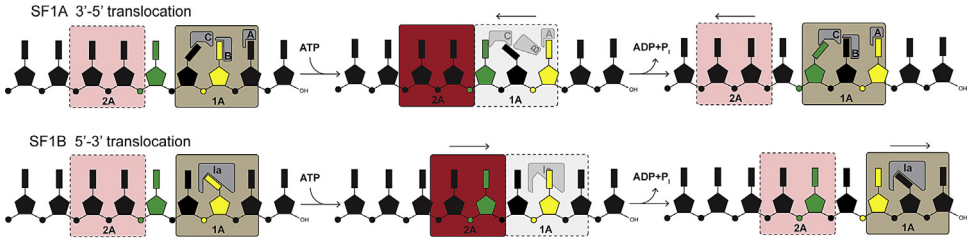

Fig. 3. Mechanistic models of helicase translocation with different polarities. Schematic representation of major conformational changes upon ATP binding and hydrolysis based on crystal structures of PcrA (top) and RecD2 (bottom). Domains with the relatively weaker binding affinity are depicted in lighter colors and with dashed lines. Mechanistic details are explained in the accompanying Section 2.3.

account for strand separation when the helicase reaches a double-stranded region simply by excluding the other strand from entering the binding site and prying the duplex open. In fact, the amount of energy released by hydrolysis of any NTP (~10 kcal/mol) should be more than sufficient to separate an average base pair under physiological conditions (~1.6 kcal/mol) (von Hippel and Delagoutte, 2001). Still, the question whether the actual unwinding is actively supported by the protein or occurs passively depending on thermal fraying, that is, spontaneous opening and closing, of double strands is still an unresolved issue. In order to clarify the use of active and passive in this respect, it should be made clear that this terminology relates to the mechanism by which strand opening is achieved and not to the overall enzyme activity, which is by definition always active in the biochemical sense as it requires NTP hydrolysis.

In a passive unwinding model, the helicase would temporarily pause when it encounters a double-stranded region and move forward once the base pair opens, thereby preventing re-annealing of the single strands (Lohman and Bjornson, 1996). Although estimates on the fraying frequency are as high as 1000 s^{-1}, this model would not account for helicase proteins or complexes that possess higher unwinding rates, for example RecBCD (Chen et al., 1992; Liu et al., 2013). Thus, at least some helicases seem to employ an active mechanism for duplex destabilization (Pyle, 2008; Singleton and Wigley, 2002). Support for such a mechanism was again obtained from the crystal structure of PcrA (Velankar et al., 1999). In this case the optional domains 1B and 2B play a critical role by specifically binding to double-stranded DNA in the context of the NTP-bound state. Once the NTP is hydrolyzed, their binding affinity is lost, and contacts with the DNA are predominantly limited to both core domains. Thus, NTP binding does not only start translocation, it also leads to the bending of the duplex region behind the fork. As a consequence of this distortion, the first four to five base pairs at the junction start to open, which allows stabilization of the newly generated single-stranded region by the forward motion of the protein.

In contrast to the duplex opening, the translocation mechanism described with the inchworm model implies that PcrA progresses by a single base per NTP hydrolyzed. Therefore, it is possible that translocation and unwinding are not coupled during every hydrolysis cycle in PcrA (Velankar et al., 1999), a hypothesis that would also explain unwinding step sizes of more than one base pair seen with some other helicases. This theoretical concept was supported by findings for HCV NS3, which suggested that three successive hydrolysis events trigger the sudden unwinding of three base pairs in a so-called spring-load mechanism (Myong et al., 2007). Thus, it is important to distinguish between translocation step size, which may be fixed at one nucleotide per NTP, and the size of individual unwinding steps, which may involve hydrolysis of several NTP molecules.

From the study of multiple members of different helicase superfamilies, it has now become apparent that introduction of some kind of mechanical strain into the double-stranded region, to ease its opening up, may be a common part of helicase action. However, as the participation of non-conserved domains already implies, the exact mechanism of strand separation may vary between helicases. Particularly, the element responsible for the destabilization, called pin or wedge, may be part of different domains and vary in size (Saikrishnan et al., 2008; Singleton et al., 2001, 2004; Velankar et al., 1999).

3. The nidovirus helicase: a multi-functional enzyme controlling key steps in viral replication

The presence of a helicase in nidoviruses was recognized already in the late 1980s by comparative genomics involving the first sequenced nidovirus genome, that of the avian infectious bronchitis coronavirus (Boursnell et al., 1987), along with known bacterial helicases, for example UvrD. These findings led to the original proposal to establish SF1, the first among helicase superfamilies, and to classify the corresponding nidovirus protein domain as putative helicase (Gorbalenya et al., 1988, 1989b; Hodgman, 1988). Subsequent genomic studies of other nidoviruses reported conservation of this domain and its characteristic helicase motifs, strongly supporting the helicase function in nidoviruses.

The multidomain helicase subunit (hereafter referred to as helicase) of nidoviruses ranges in size from 50 to 70 kDa and is called nsp10 in arteriviruses and nsp13 in coronaviruses, which are the only nidovirus families that were characterized in respect of this enzyme. The protein is encoded in replicase ORF1b and proteolytically released from a non-structural polyprotein (pp1ab) that results from ORF1a/1b ribosomal frameshifting (Fig. 4). Comparative sequence analysis indicated that the nidovirus helicase subunit consists at least of an N-terminal zinc-binding domain (ZBD; known also as Zn-binding module, Zm, or complex Zn-finger), the helicase core domains, and an as yet undefined C-terminal part. Despite considerable size differences, it is one of the three ubiquitous and evolutionary most conserved proteins encoded by nidoviruses. The other two are the chymotrypsin-like protease (3CL^{pro} or main protease M^{pro}), responsible for most of the proteolytic processing of pp1a and pp1ab, and the RNA-dependent RNA polymerase (RdRp) that is thought to synthesize the genome as well as a set of subgenomic (sg) mRNAs (Gorbalenya et al., 2006; Lauber et al., 2013). The helicase is genetically segregated with the RdRp in ORF1b and mutation of specific conserved residues can either negatively impact or block replication of the arterivirus equine arteritis virus (EAV) (Seybert et al., 2005; van Dinten et al., 2000), the only nidovirus for which reverse genetics analysis of the helicase was performed so far. These genetic and genomics observations established the helicase as an essential protein for viral replication.

Biochemically, helicase activity was first demonstrated for a coronavirus and an arterivirus (Seybert et al., 2000a,b) just few years before the 2003 SARS (severe acute respiratory syndrome) pandemic, which sparked renewed interest in nidoviruses in general and coronaviruses in particular. By now biochemical data are

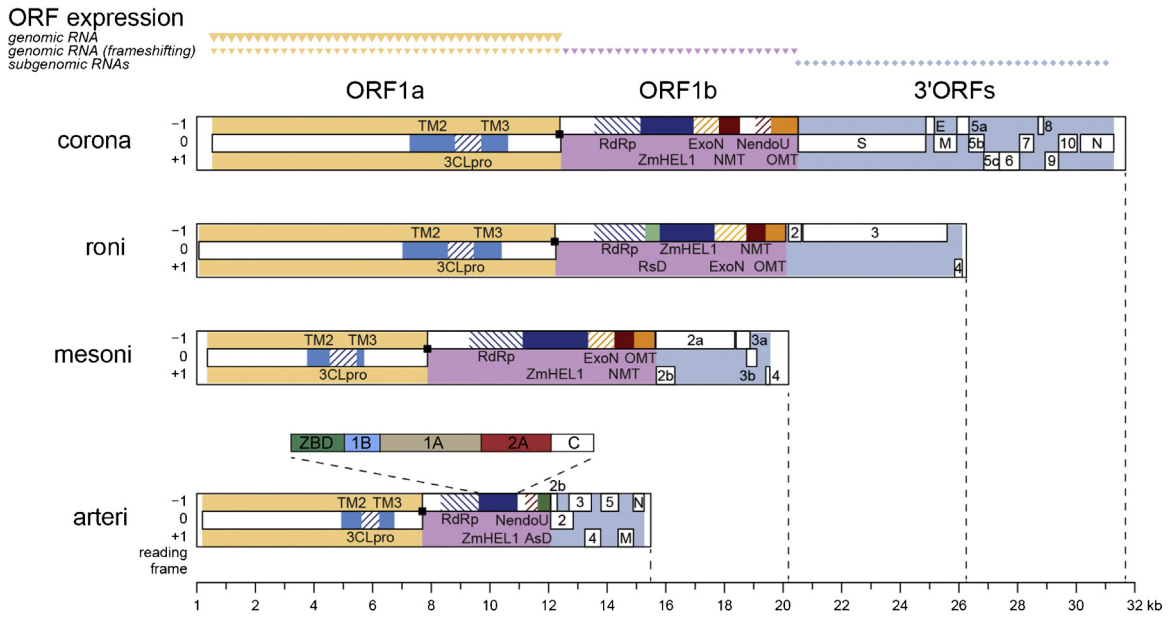

Fig. 4. Genomic organization and key replicase domains of four nidoviruses. The coding regions are partitioned into ORF1a (yellow), ORF1b (purple), and the 3′ ORFs (blue), which also differ in their expression mechanism or template as indicated on top. Black squares, ribosomal frameshift sites. Within ORFs (white rectangles), colored patterns highlight domains identified in: all nidovirus replicases [transmembrane domain 2 (TM2), transmembrane domain 3 (TM3), 3C-like protease (3CLpro), RNA-dependent RNA polymerase (RdRp), and Zn-binding domain fused with helicase domain (ZmHEL1)], light and dark blue; large nidoviruses [exoribonuclease (ExoN), 2′-O-methyltransferase (OMT)], orange; certain clades [N^7-methyltransferase (NMT), endoribonuclease (NendoU)], red; ronivirus-specific domain (RsD), light green; arterivirus-specific domain (AsD), dark green. Genomic organizations are shown for Beluga whale coronavirus SW1 (corona), gill-associated virus (roni), Nam Dinh virus (mesoni), and porcine respiratory and reproductive syndrome virus, North American genotype (arteri). Domain organization of ZmHEL1 is shown for arteriviruses.
Adapted from Lauber et al. (2013).

available for helicases originating from severe acute respiratory syndrome coronavirus (SARS-CoV) (Adedeji et al., 2012a; Ivanov et al., 2004; Lee et al., 2010; Tanner et al., 2003; Thiel et al., 2003), human coronavirus 229E (HCoV-229E) (Ivanov and Ziebuhr, 2004; Seybert et al., 2000a; Seybert and Ziebuhr, 2001), porcine reproductive and respiratory syndrome virus (PRRSV) (Bautista et al., 2002), and EAV (Seybert et al., 2000b, 2005; Deng et al., 2014). Furthermore, as mentioned above the latter was also extensively probed in reverse genetics studies (Seybert et al., 2005; van Dinten et al., 2000), and the crystal structure of a truncated variant was reported recently (Deng et al., 2014). In contrast, putative helicases originating from the invertebrate families *Roniviridae* and *Mesoniviridae* have not been experimentally characterized calling for caution with respect to generalization of results available exclusively for vertebrate nidoviruses. For the sake of clarity, the source of the described data, that is either from an arterivirus or a coronavirus, is stated throughout this paper unless a general conclusion applicable to all vertebrate nidoviruses is drawn.

3.1. Three different enzyme activities with contrasting substrate requirements

3.1.1. A promiscuous NTPase sensitive to the presence of polynucleotides

As discussed in Section 2, helicase translocation is driven by the energy released upon hydrolysis of phosphodiester bonds of NTPs. Accordingly, mutation of the conserved lysine of motif I (G/A)x(A/P)GxGK(S/T), which binds ATP, abolished all NTPase activity of the nidovirus helicases probed thus far (Ivanov et al., 2004; Ivanov and Ziebuhr, 2004; Seybert et al., 2000a,b). Additionally, a number of labs characterized the nucleotide specificity of these proteins (Bautista et al., 2002; Ivanov et al., 2004; Ivanov and Ziebuhr, 2004; Tanner et al., 2003). However, a direct comparison of the kinetic constants obtained in these studies is complicated by different experimental conditions used regarding pH, incubation temperature, and presence of homopolymeric RNAs.

In general, like the SF1 helicases of the alphavirus-like viruses CHIKV nsP2 (*Togaviridae*) (Das et al., 2014) and HEV ORF1 protein (*Hepeviridae*) (Karpe and Lole, 2010a), none of the nidovirus enzymes tested seemed to be able to strongly discriminate between any of the ribo- or deoxynucleotides. EAV nsp10 was found to utilize both tested nucleotides, ATP and GTP, with comparable efficiency (Seybert et al., 2000b). Similarly, PRRSV nsp10 was able to hydrolyze all NTPs with a preference for purines over pyrimidines and with UTP being the least favorite substrate (Bautista et al., 2002). The same order of substrate preferences was deduced in one SARS-CoV nsp13 study, where the obtained k_{cat}/K_m values ranged from 1.9 $\mu M^{-1}\,s^{-1}$ for ATP and GTP to 0.4 $\mu M^{-1}\,s^{-1}$ for UTP (Ivanov et al., 2004). Yet, a second study by Tanner et al. (Tanner et al., 2003) on the same protein carrying a different affinity tag reported an almost twofold difference between ATP (k_{cat}/K_m = 57.9 $mM^{-1}\,s^{-1}$) and GTP (k_{cat}/K_m = 27.0 $mM^{-1}\,s^{-1}$) but a similar efficiency for GTP and CTP (for a discussion of the influence of affinity tags and choice of expression system on enzyme activities see below). Again UTP was the least efficiently used substrate (k_{cat}/K_m = 19.1 $mM^{-1}\,s^{-1}$). However unlike other studies, the latter research was performed in the presence of a polynucleotide, polyuridine (polyU). As such homopolymeric co-factors are known to affect the NTPase rate of a number of helicases (Bhattacharya et al., 2000; Bird et al., 1998; Preugschat et al., 1996), this difference in experimental set-up may explain the observed variation in the relative order of substrate preference (see also below). Finally, also the HCoV-229E helicase behaved similarly in terms of NTP selectivity, with again ATP being the most and UTP the least preferred substrate (k_{cat}/K_m = 0.9 $\mu M^{-1}\,s^{-1}$ and 0.3 $\mu M^{-1}\,s^{-1}$, respectively) (Ivanov and Ziebuhr, 2004). Furthermore, besides the differences observed in the two SARS-CoV nsp13 studies, for which a possible

reason was discussed above, all groups examining coronavirus helicases reported that different dNTPs and NTPs could be utilized with the same overall relative preference. What discriminated them was an up to threefold lower efficiency of the utilization of dNTPs compared to NTPs. Given the general resemblance between the data obtained with helicases of selected coronaviruses and arteriviruses, it is tempting to speculate that this lack of specificity is conserved in these two distantly related families of vertebrate nidoviruses. It remains unknown whether this property may also be conserved in the invertebrate nidoviruses whose helicases have not been characterized at all.

Interestingly, the observations described above suggest that neither base-specific side chains nor the 2′-OH contribute significantly to nucleotide binding. Instead, the mere presence of a 5′ triphosphate may be the sole prerequisite for promoting NTPase activity. This interpretation is further supported by a three-dimensional model of the highly conserved helicase core domains 1A and 2A of SARS-CoV nsp13, computed by Hoffmann et al. (Hoffmann et al., 2006) based on structures of the PcrA, Rep, and RecB DNA helicases. After molecular dynamics simulation and energy minimization of ATP binding, six hydrogen bonds between the β- and γ-phosphates of the ATP and the side chains of (partially) conserved residues (T286 motif I, K288 motif I, R443 motif IIIa, R567 motif VI) were predicted. Moreover, an additional hydrogen bond may be established between the 3′-OH of the sugar and E540 (motif Va). Additionally, the base may be involved in a stacking interaction with H290 (extended motif I) and a cation–π interaction with R442 (motif IIIa). In contrast, no interactions that would be specific for the adenine base could be identified. Finally, a hydrogen bond was predicted to be present between the 2′-OH of the ribose and K569 (motif VI). With respect to the experimental data, the presence of this single interaction, as compared to the nine interactions that are not specific for the type of sugar, may explain the only slight reduction of enzymatic activity when using deoxynucleotide substrates.

In Section 2, we mentioned the stimulation of the NTPase activity of eukaryotic and bacterial SF1 and SF2 helicases by single-stranded nucleic acids. This effect was also observed for the nidovirus helicases of SARS-CoV, HCoV-229E, and EAV (Seybert et al., 2000a,b; Tanner et al., 2003). All studies recorded the strongest stimulation by poly(U), poly(dT), and poly(dA). A remarkable finding was the unusual magnitude of the increase, 15- to 20-fold for EAV, 15- to 25-fold for SARS-CoV, and ∼50-fold for HCoV-229E, which is similar to the enhancement observed for viral SF2 helicases, like HCV NS3, which could be stimulated up to 15-fold (Kadare and Haenni, 1997; Suzich et al., 1993). In contrast, the nucleic acid-stimulated enhancement of NTP hydrolysis by SF1 helicases of viruses of the alphavirus-like supergroup was generally found to be minor, mostly about twofold (Das et al., 2014; Gros and Wengler, 1996; Kadare et al., 1996; Karpe and Lole, 2010a). SARS-CoV nsp13 helicase activity was furthermore stimulated by more than 15-fold by poly(A) and poly(dC). While HCoV-229E nsp13 activity was also significantly increased by the presence of poly(C) (32-fold), neither poly(A), poly(G), nor tRNA induced a more than fivefold stimulation. Similarly, EAV nsp10 NTPase activity was only enhanced up to fourfold by tRNA and homopolymeric RNAs other than poly(U). The observed variation in the scale of stimulation of NTPase activity depending on the type of polynucleotide raises the question of its molecular basis. On the one hand, it could merely reflect a higher affinity for certain nucleic acid substrates compared to others, which would imply sequence-dependent helicase activity. Yet, as the affinity toward nucleic acids has not been evaluated for any of the nidovirus helicases so far and little is known about the exact means by which these allosteric activators may influence NTPase activity, alternative explanations should also be considered. For instance, based on crystal structures of HCV NS3, Frick et al. (2004) suggested that electrostatic changes inside the NTP-binding site could be caused by a subtle rotation of domain 2A upon nucleic acid binding. From computer simulation of the ionization states of amino acid side chains, it appeared that this conformational change would lead to a switch of the protonation states of the conserved lysine in motif I and the conserved aspartate of motif II and would thus directly influence the NTPase rate. Therefore, the magnitude of nucleic acid stimulation may be indirectly governed by the relay of conformational changes from the nucleic acid binding channel in the vicinity of domains 1A and 2A to the NTP binding cleft between these domains. In this line of reasoning, different nucleic acids may differ in respect to their ability to induce conformational changes rather than their binding affinity, a property which might be also relevant for nidovirus helicases.

3.1.2. A DNA and RNA helicase with stringent requirements for its partially double-stranded substrate

3.1.2.1. A helicase without nucleic acid preference. After confirmation of their NTPase activity, the next question was whether the putative nidovirus helicases are indeed functional and capable of unwinding nucleic acid duplexes, presumably the double-stranded RNAs that are formed during viral replication. HCoV-229E nsp13 and EAV nsp10 were the first proteins for which this question was addressed in a so-called “all-or-nothing” assay, which only records unwinding events that result in complete strand separation (Seybert et al., 2000a,b). In these pioneering studies, published in short succession by Seybert et al., both proteins were able to unwind not only partially double-stranded RNA but also DNA substrates containing a single-stranded region at one or both of the 5′ ends, irrespective of the additional presence of 3′ tails. In contrast, no activity was observed with substrates containing only an unpaired region at one of the 3′ ends or with blunt-ended substrates. These findings demonstrate that the nidovirus helicase recognizes and binds single-stranded RNA and DNA (see section 3.2 for the structural basis for this lack of specificity) before proceeding to unwind in 5′–3′ direction. Later, the same polarity was also established for SARS-CoV nsp13 (Ivanov et al., 2004; Lee et al., 2010; Tanner et al., 2003) and PRRSV nsp10 (Bautista et al., 2002), confirming the classification of nidovirus helicases as members of SF1B. In comparison, the helicases of CHIKV nsP2 and HEV ORF1 protein did share the 5′–3′ polarity on RNA substrates but were incapable of unwinding DNA (Das et al., 2014; Karpe and Lole, 2010a), indicating that these properties could be uncoupled.

The assays employed in the initial studies mentioned above were based on a multiple-turnover approach, which assesses and compares the ratio of single-stranded products to double-stranded substrates at a defined reaction end point. Therefore, they disregard multiple unwinding events involving the same substrate but different helicase molecules and, in these particular studies, also product re-annealing (Seybert et al., 2000a,b). Thus, differences in binding affinity, processivity, and velocity of the enzyme when comparing the two substrates may have been masked. Addressing the basis of the apparent lack of substrate specificity, the unwinding kinetics of RNA and DNA substrates with identical sequences have been examined more closely for SARS-CoV nsp13 using a single-cycle assay, which prevents re-binding of proteins that have dissociated from the nucleic acid or that are not bound when the reaction is started by ATP addition (Adedeji et al., 2012a). Strikingly, also in this single-turnover experiment no difference was observed between the unwinding of RNA and DNA substrates. On the one hand, this lack of specificity may reflect a structural property (see Section 3.2) that has evolved due to the lack of selection for discriminating between the two substrates and thus has no immediate functional implications for the virus. On the other hand, while RNA unwinding may be employed during replication and/or transcription of viral RNAs, the helicase could specifically exert its DNA unwinding

activity on host nuclear DNA as proposed for the SF2 helicase of HCV, which even showed a preference for DNA over RNA substrates in absence of protein co-factors (Pang et al., 2002). However, no nidovirus helicase was found to be traveling to the nucleus, which stands in contrast to a few other non-structural proteins, for example nsp1 of EAV (Tijms et al., 2002). Alternatively, the hypothesis could be modified to propose that the nidovirus helicase might target host mitochondrial DNA, a possibility that has not been discussed in the literature to the best of our knowledge. Finally, the biochemical properties described above were determined using *in vitro* assays utilizing purified recombinant helicases and may be only partially applicable to helicases within viral replication complexes, which include other proteins and co-factors.

3.1.2.2. The influence of sequence and size of single-stranded nucleic acids on helicase activity and oligomeric state. Next to the nature of the sugar, the sequence of the single-stranded region used to initially bind the protein may provide specificity for certain substrates. Therefore, again Seybert et al. (2000a) investigated the unwinding of DNA duplexes containing 10-nt long homopolymeric tails at one of their 5′ ends. Although HCoV-229E nsp13 could utilize substrates with a dA, dC, or dT tail, it showed a marked preference for the two pyrimidines. In contrast, dG-containing duplexes were not unwound. However, this may not be due to a specific discrimination against guanine but rather to the formation of higher order structures in this particular substrate, which, as the authors speculated, may interfere with helicase activity. Later, it was also demonstrated that SARS-CoV nsp13 is able to initiate unwinding on tails with random sequences (Adedeji et al., 2012a). Despite this apparent lack of sequence specificity in these *in vitro* assays, the function of the nidovirus helicase in infected cells may require loading at specific nucleic acid sequences or higher-order structures. Thus, it would be interesting to investigate binding affinities toward, for example, sequences located within the untranslated region of the genome, the antigenome, or any of the transcription-regulating sequences (TRSs) that direct the production of nidoviral sg RNAs (see Section 3.3.2). Furthermore, it is conceivable that one (or more) of the other non-structural proteins may interact and target the helicase to specific genome regions if it indeed would not possess any specificity itself.

In addition to the sequence, also the length of the 5′ overhang is important for binding of the protein to its nucleic acid substrate. Besides revealing the minimal spatial requirements for helicase binding, characterization of this property may more importantly provide functional insights into the still disputed matter concerning the need for dimerization of SF1 helicases, which possibly leads to cooperativity. However, it should be noted that the NTP-binding motifs of the two SF1 core domains face each other to form an intact NTP-binding site in each protein subunit. Therefore, proteins of this superfamily are not *per se* dependent on oligomerization. In contrast, in SF3-6 members, whose binding motifs are localized on distant sides of the protein, assembly of a functional NTP binding site requires two subunits (Singleton et al., 2007). Nevertheless, it has been shown for individual SF1 members that dimerization is required at different stages of the enzymatic cycle. For instance, the *E. coli* helicase UvrD requires dimerization to initiate and sustain unwinding but not to translocate along DNA (Ali et al., 1999; Fischer et al., 2004; Maluf et al., 2003; Maluf and Lohman, 2003).

To shed light on the oligomerization requirements of nidovirus helicases, unwinding of DNA substrates with the same double-stranded region but progressively shorter tails was tested for SARS-CoV and HCoV-229E nsp13 (Adedeji et al., 2012a; Lee et al., 2010; Seybert et al., 2000a). In agreement with the results summarized above, unwinding was observed in all studies if the DNA contained an overhang of ten or more nucleotides. In contrast, the results of experiments using substrates with shorter 5′ overhangs and SARS-CoV nsp13 were less consistent between different groups but suggested that the minimal length required for binding may be in the range of five to seven nucleotides. However, it is important to note that all factors that may influence the extent and frequency of the fraying of the double-stranded part of the substrate, like temperature, sequence, or salt concentration, may have influenced the outcome of these experiments.

Given the need for only short binding sequences, it is possible that multiple helicase molecules bind simultaneously to a single substrate molecule with a longer tail region, giving rise to cooperativity effects. Interestingly, the data from Lee et al. (2010) suggests that such a scenario could be possible for nidovirus helicases. While unwinding of DNA comprising a 50-base pair duplex region and tails of 15 or less nucleotides was inefficient (<7.5% unwound) in a single-cycle all-or-nothing assay containing a 40-fold excess of protein over DNA, the ratio of single-stranded to double-stranded DNA increased stepwise to 18%, 55%, and 95% when the tail was extended to 20, 30, or 40 nt, respectively. Although this result could also be explained by an increasing affinity between a single protein and its substrate and therefore by more frequent initiation of unwinding, the absence of a direct correlation between tail length and activity makes it tempting to speculate that a second molecule entered the reaction once the tail exceeded a certain length, most likely 20 nt (Lee et al., 2010). Additionally, in the same study it was shown by cross-linking experiments with DMS (dimethyl suberimidate) that SARS-CoV nsp13 can form dimers, trimers, and possibly also larger oligomers in solution in the absence or presence of ATP and DNA. Notwithstanding a possibility of forming artificial oligomers by aggregation, this finding would, at least in principle, be consistent with an earlier yeast-two-hybrid screen indicating a SARS-CoV nsp13 self-interaction (von Brunn et al., 2007). Nevertheless, none of the studies has addressed the question whether helicase molecules indeed form oligomers during unwinding. Likewise, it is unknown whether oligomer formation affects biophysical properties of the individual monomers to reveal typical indicators of cooperativity, such as coordinated substrate binding or translocation activities (Levin et al., 2004). Accordingly, Lee et al. (2010) postulated that the higher net product formation is plausible if at least one of the independently operating helicase molecules stayed attached to the substrate until unwinding was completed.

3.1.2.3. The size of double-stranded regions of the substrate affects helicase processivity. The fact that a comparable tail length-dependent increase of unwinding was not observed in two other studies using a similar design but employing polynucleotides with slightly shorter duplex regions underlines the importance of another feature of helicases, their processivity. This feature is defined as either the average number (N) of base pairs that a helicase can unwind without dissociating from its substrate or as the probability (P) that a helicase proceeds with unwinding after each catalytic cycle. This property should not be mistaken for rate of translocation that is defined as number of base pairs unwound per second (Lohman and Bjornson, 1996). In general, processivity can be influenced in two ways; first, by the protein's affinity for a nucleic acid, and second, by preventing re-annealing of freshly separated strands. The latter can be achieved by simultaneous binding of additional proteins behind the helicase irrespective of having a physical interaction with it. Additionally, this would also reduce the rate of backward movement, called slippage (Manosas et al., 2010). Thus, the mere presence of a second nsp13 molecule, as opposed to true biochemical cooperativity, could also explain the data obtained by Lee et al. (Lee et al., 2010) with duplexes containing successively longer tails.

To assess the processivity of the SARS-CoV helicase, DNA substrates with a 20-nt tail and increasingly longer double-stranded parts were assayed in single-cycle experiments. As expected, the

percentage of unwound double strand decreased with increasing duplex length (Adedeji et al., 2012a; Lee et al., 2010). After correction for spontaneous melting of the last eight to ten base pairs, which is frequently observed in the presence of helicases (Eoff and Raney, 2006), Adedeji et al. calculated a processivity (expressed as probability) of 0.80 ± 0.03, which appears to be surprisingly low given the 32-kb genome size of SARS-CoV (Adedeji et al., 2012a). With this value nsp13 would rank far below the highly processive *E. coli* heterotrimeric complex RecBCD (processivity ~1), which contains two functional SF1 helicases, but slightly above T4 phage Dda with a processivity of 0.73 (Eoff and Raney, 2006; Lucius et al., 2002) that unwinds a dsDNA genome of a size comparable to that of coronaviruses. However, in the context of a viral replication complex this processivity may be substantially higher due to an increase of the overall affinity of the complex toward RNA and prevention of re-annealing. The kinetic step size, defined as the number of base pairs separated per enzyme cycle, hence not necessarily per NTP hydrolyzed, was estimated to be 9.4 ± 2.1 bp. The catalytic rate for unwinding of DNA was determined to be 30 steps per second (Adedeji et al., 2012a). No parameters were calculated by Lee et al. (2010).

Strikingly, although comparable DNA substrates were used in both studies (Adedeji et al., 2012a; Lee et al., 2010), the unwinding kinetics differed substantially. In one case the fraction of unwound substrate plateaued after approximately 100 to 500 s (Lee et al., 2010), while in the other it took less than 1 s (Adedeji et al., 2012a) for all duplex lengths. Conveniently, the authors of the latter study also provided the explanation for this difference when they compared three different recombinant nsp13 fusion proteins containing either a GST (glutathione S-transferase), MBP (maltose-binding protein), or hexahistidine moiety at their N-termini (Adedeji et al., 2012a,c). Besides the fusion partner, a second difference was that the GST version was expressed in eukaryotic cells with the help of a baculovirus vector, while the other two were expressed in *E. coli*. Similar to the his-tagged bacterially expressed protein from Lee et al., they found a several hundred-fold lower ATPase rate compared to GST nsp13 originating from baculovirus ($0.2\ s^{-1}$ compared to $104.1\ s^{-1}$) for proteins which were expressed in *E. coli*, regardless of the tag used. At the same time, however, DNA binding properties remained unaffected. When considering this difference, it is interesting to note that neither the GST nor the MBP moiety could be removed from SARS-CoV nsp13, nor the His tag from its HCoV-229E homolog (Adedeji et al., 2012a; Ivanov et al., 2004; Seybert et al., 2000a). This may suggest that each of these foreign sequences was similarly closely associated with the N-terminal domain of the viral protein and hence inaccessible for a protease. Thus, it seems likely that not the identity of the foreign sequence was the cause of the inhibition in the study by Lee et al. (Lee et al., 2010) but rather the expression in a bacterial host that may have resulted in misfolding. Therefore, the numbers cited above should be taken with caution and the design of any future experimental studies seeking to determine biophysical parameters of nidovirus helicases should take this effect into account.

3.1.3. RTPase: an enzymatic activity not required for helicase function

Many RNA viral helicases of SF1 and SF2 were shown to possess RNA 5′-triphosphatase (RTPase) activity, that is, the capability to specifically cleave the phosphodiester bond between the β- and γ-phosphate of the most 5′ nucleotide of newly synthesized RNA (Balistreri et al., 2007; Benarroch et al., 2004; Karpe et al., 2011; Karpe and Lole, 2010b). This activity was shown to be the first of four consecutive steps in the conventional RNA capping pathway (reviewed in (Decroly et al., 2012)), leading to the addition of an m^7GpppNm-cap to the 5′ end of mRNA. It is employed for mRNA capping by all eukaryotes and, presumably, also by a number of RNA viruses with capped genomes, for example flaviviruses and alphaviruses utilizing their NS3 and nsP2 helicases, respectively (Benarroch et al., 2004; Karpe et al., 2011). To test whether this activity is also shared by the helicases of nidoviruses, which also employ capped genomes (Lai et al., 1982; Sagripanti et al., 1986; van Vliet et al., 2002), short RNA substrates were *in vitro* transcribed in the presence of [γ-^{32}P]GTP. After incubation with SARS-CoV or HCoV-229E nsp13 (Ivanov et al., 2004; Ivanov and Ziebuhr, 2004) or most recently EAV nsp10 (our unpublished data), the radioactive phosphate was released, while the RNA stayed otherwise intact. Conversely, when the same assay was performed with RNAs transcribed in the presence of [α-^{32}P]GTP, neither helicase was able to release the radioactive label, indicating that they do not possess general phosphatase activity. As, from a mechanistic perspective, the RTPase activity is very similar to the already reported NTPase activity, the next question was whether both activities would utilize the same active site. To this end, an alanine substitution mutant of the conserved lysine located in motif I was shown to abolish both NTPase and RTPase activities for the above mentioned coronaviruses (Ivanov et al., 2004; Ivanov and Ziebuhr, 2004). Thus, the authors concluded that the utilization of both substrates depends on the same active site. To further support this conclusion, competition experiments between both activities were performed. In agreement with their conclusion, ATP acted as potent inhibitor for RTPase activity, while AMP had almost no effect. These results imply that nidovirus helicases may also be involved in the control of the translation of their mRNAs.

3.2. Structure: interplay between enzyme core, ZBD and a new accessory domain revealed upon polynucleotide binding

Recently, EAV nsp10 became the first nidovirus helicase (and only the second RNA viral SF1 helicase after that of ToMV (Nishikiori et al., 2012)) for which a three-dimensional structure was reported (Deng et al., 2014). The structure was solved for a somewhat truncated version of the helicase, which did not include the most C-terminal 65 amino acid residues, after the full-length protein failed to form any crystals. This truncation did not involve any of the conserved helicase motifs, and neither ATPase nor helicase activity were abolished, supporting the relevance of the structure of this truncated nsp10 version. In fact, compared to the full-length wild-type protein, this engineered protein variant showed an increased ATPase activity in the absence of homopolymeric RNA. Nevertheless, its unwinding activity seemed to be moderately lower than for the full-length protein, indicative of less efficient coupling between ATPase and helicase activities. This may suggest that the C-terminal domain, which is not conserved among nidoviruses, is not only flexible but perhaps also exerts a regulatory function on the helicase core, facilitating coupling between NTPase and polynucleotide binding activities.

Overall the EAV nsp10 structure revealed an organization comprising four domains successively encoding: an N-terminal ZBD, a new domain designated 1B, and two RecA-like domains (1A and 2A, together designated HEL1) containing all conserved helicase motifs in line with prior analyses (Hodgman, 1988; Gorbalenya et al., 1988; Fairman-Williams et al., 2010). In comparison to representative members of the three SF1 helicase families, this organization is most similar to that of Upf1, which contains three accessory domains, an N-terminal zinc-binding domain followed by 1B, and 1C inserted into the 1A core domain (Cheng et al., 2007). In contrast, UvrD and RecD2 of the UvrD/Rep and Pif1-like families, respectively, comprise insertions, designated 1B and 2B, in both core domains. While these insertions are the only additional domains for UvrD, RecD2 also features an N-terminal domain that, however, does not include a zinc-finger (Fig. 5) (Lee and Yang, 2006; Saikrishnan et al., 2009). At this point, it is important to note that

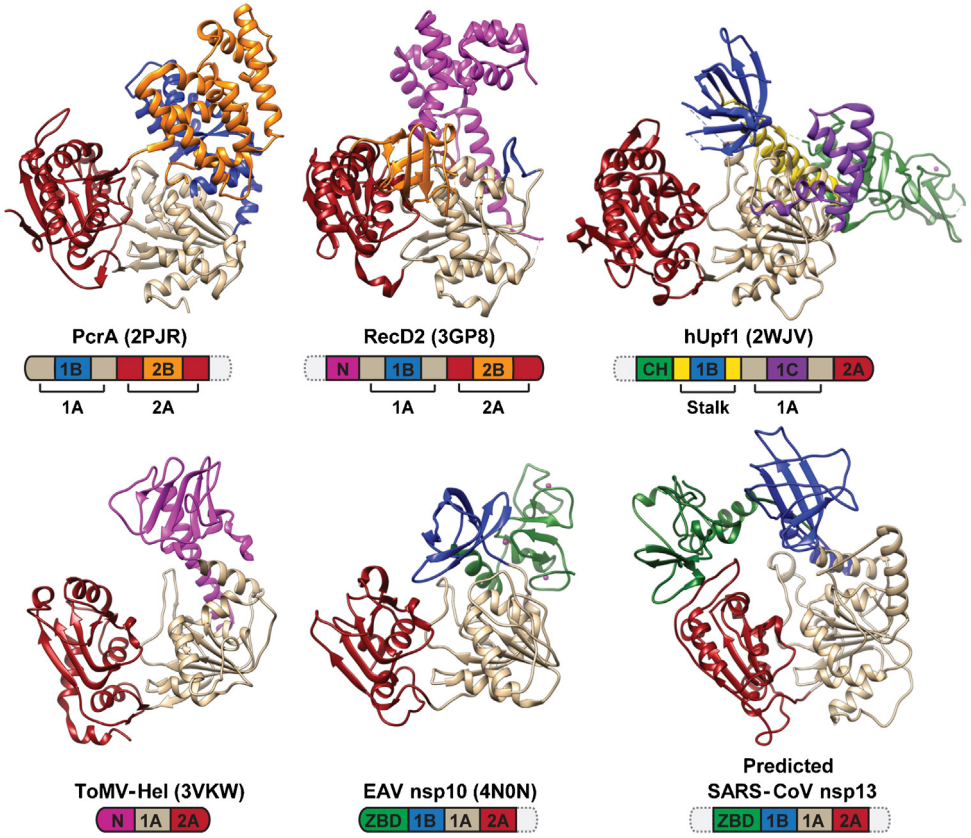

Fig. 5. Three-dimensional models of prototypic prokaryotic and eukaryotic (top) and viral (bottom) SF1 helicases. Depicted are the prototypic helicases PcrA (UvrD/Rep family), RecD2 (Pif1-like family), hUpf1 (Upf1-like family), as well as the currently only available structures of viral SF1 helicases of tomato mosaic virus (ToMV) and equine arteritis virus (EAV). Also shown is a structure prediction of severe acute respiratory syndrome coronavirus (SARS-CoV) nsp13 obtained with Phyre2 (Kelley and Sternberg, 2009). Based on sequence and structural comparisons nidovirus helicases are classified into the Upf1-like family. Domain colors correspond to those used for the domain organization schemes depicted below each structure. Same coloring of domains other than 1A and 2A does not imply any evolutionary relationship. Zn^{2+} ions are depicted as pink spheres. Dashed domains in the organization schemes represent parts that could not be modeled. Domain sizes are not to scale. PDB accession numbers are listed in brackets.

an equivalent designation does not imply a divergent evolutionary relationship of accessory domains if these domains are associated with distantly related helicases.

Domain 1A (residues 138–293) of the EAV nsp10 structure folds as a parallel five-stranded β-sheet sandwiched between three and two α-helices on the sides. Conversely, domain 2A (residues 294–401) is comprised of a parallel four-stranded β-sheet and five α-helices facing domain 1A. Comparison of the domain structure with all protein structures currently available yielded the closest similarity to the SF1B helicase Upf1 and its close homolog Ighmbp2 with *Z*-scores of 20.9 (RMSD 3.5 Å) and 19.9 (RMSD 3.0 Å), respectively. Likewise, the newly discovered 1B domain (residues 83–137), which contains a two- and a three-stranded antiparallel β-sheet arranged into a β-barrel fold, resembles a domain found in the Upf1-like helicase subfamily in terms of its location and orientation relative to the helicase core and was thus named accordingly. Finally, the ZBD (residues 1–82) coordinates three zinc ions with its twelve conserved cysteine and histidine residues and folds as two distinct zinc-binding modules, which are connected by a disordered region (Fig. 6). The larger N-terminal module (residues 1–40) coordinating two zinc ions can be classified as RING-like with a binuclear structure with cross-brace topology. Within this structure a treble-clef zinc finger-like motif, involving four cysteines in the case of EAV nsp10, chelates the first metal ion, while the second ion is embedded in an αββ zinc finger-like motif containing two cysteines and two histidines in EAV nsp10. Based on nidovirus-wide sequence conservation the signature residues of this RING-like motif can be described with the formula $Cys2_A$-Cys_B-Cys_A-$[His/Cys]_A$-$[His/Cys]3_B$ (with A and B designating the chelated zinc ions, residues in brackets indicating alternative amino acids, and numbers indicating the number of times the residue occurs in succession). The more distal zinc-binding module (residues 41–65), which is built by three cysteines and one histidine in EAV, has a treble-clef fold that is different from the one of the RING module. Its conservation pattern can be described as Cys-[His/Cys]-Cys-[His/Cys]. The residues outside of these zinc-binding modules are part of either a long loop, which enables extensive hydrogen bonding with the latter module and may thus contribute substantially to the overall rigidity of the ZBD, or an α-helix connecting the zinc-binding modules with the remainder of the protein. As for the other domains, the closest similarity of the RING-like module was again found to the N-terminal and similarly complex zinc-binding CH-domain of Upf1 (*Z*-score 1.9, RMSD 2.2 Å). This similarity included structural equivalents for six of the eight chelating residues. In contrast, EAV nsp10 and Upf1 have structurally different zinc-binding modules downstream of the RING-like module, which suggests that the ZBD of nidovirus helicases prototypes a novel type of a complex multi-nuclear zinc-binding structure.

The presence and conservation of a putative complex zinc-binding domain, located between an RdRp upstream and an SF1 helicase downstream, were among the initially recognized specific features of the group of viruses, including coronaviruses and later also arteriviruses, that has now been united in the order *Nidovirales* (Den Boon et al., 1991; Gorbalenya et al., 1989a). To date, this domain has been identified as uniquely associated with all known

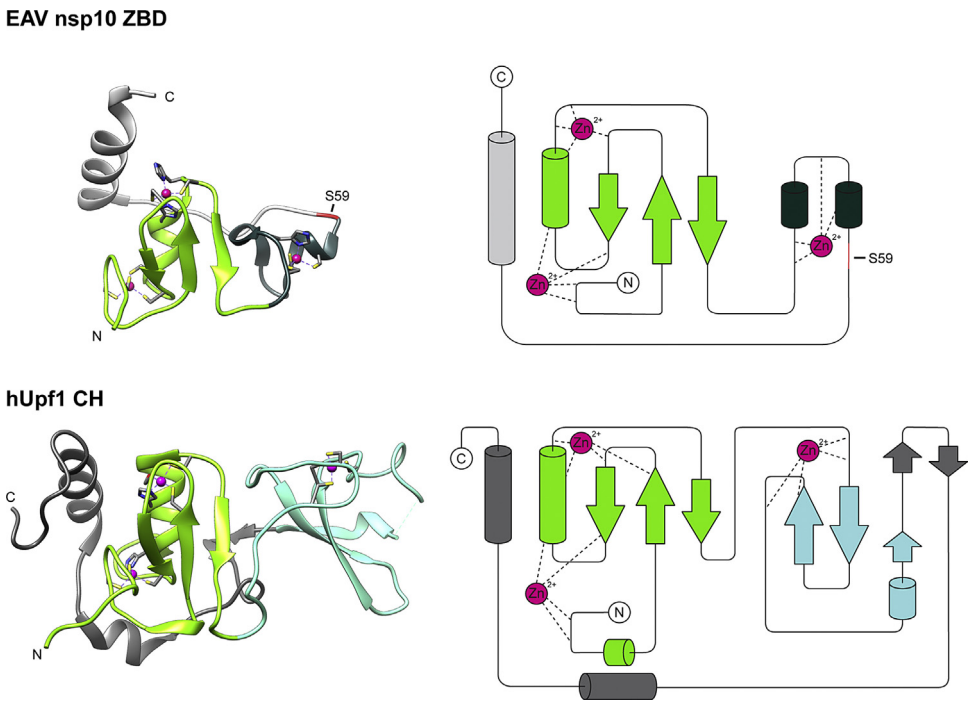

Fig. 6. Structural comparison between the EAV nsp10 ZBD and hUpf1 CH-domain. Structure and topology of the N-terminal domains of EAV nsp10 (PDB accession number 4N0N) and hUpf1 (PDB accession number 2WJV). Both domains possess a RING-like zinc-binding module of similar fold (bright green) and a second module of different fold. Linker regions are colored in light and dark gray. Residues coordinating Zn^{2+} are shown as sticks. S59 of EAV nsp10 is shown in red.

nidoviruses, which resulted in its recognition as a molecular marker of the order (Gorbalenya et al., 2006; Lauber et al., 2012). The significance of this observation for nidoviruses is highlighted by the fact that all other conserved protein or polynucleotide domains are either conserved also in other RNA viruses, *e.g.* RdRp, HEL1 or 3CLpro, or not conserved in some nidoviruses, *e.g.* NendoU or ExoN.

Interestingly, all mutant helicases expressed as N-terminal fusions to MBP were reported to have the same solubility as the wild-type protein, while His- or GST-tagged mutants clearly were less soluble (Deng et al., 2014; Seybert et al., 2005). Likewise, Seybert et al. (2005) demonstrated that zinc ions are an essential structural co-factor required for proper folding of EAV nsp10 as well as HCoV-229E nsp13. Overall, these findings support the assignment of an important role to the ZBD, which could influence the function of the helicase core by affecting its structure. The latter interpretation was further substantiated by the identification of an extensive interface area of 1019 $Å^2$ between these domains, which may be part of a signaling network (Deng et al., 2014) (see Section 3.3 for more on function).

To elucidate the basis for the lack of specificity for its nucleic acid substrate, but also to gain first insights into its potential unwinding mechanism, a second crystal structure of nsp10 was solved in complex with a partially double-stranded DNA, but in the absence of NTPs (Fig. 2C) (Deng et al., 2014). Electron density for seven of the ten thymidines of the single-stranded loading region was identified within a channel formed by domains 1A, 1B, and 2A. As biochemical data indicated, the majority of the protein DNA contacts was established either with the phosphodiester backbone or non-specifically with the base. Furthermore, none of the amino acid side chains was found to be in a position that would enable an interaction with the 2′ hydroxyl group of RNA. Although we cannot exclude that binding of an RNA substrate might induce such a contact, this structural feature may explain the lack of discrimination between DNA and RNA, which all currently tested nidovirus helicases share with some cellular members of the Upf1-like family. In agreement with the proposed unwinding model based on RecD2 (Saikrishnan et al., 2009), the 5′ and 3′ ends of the substrate were located in domain 2A and 1A, respectively. Taking the demonstrated polarity of unwinding into consideration, this implies that domain 1A must be leading during translocation. The remaining three nucleotides of the single strand as well as the double-stranded part of the substrate could not be resolved, which indicates a certain degree of flexibility of the complex. Interestingly, superposition of the C_α atoms of the helicase core domains of the free and substrate–bound structures revealed that the overall conformation of these domains is not profoundly affected by DNA binding (RMSD 0.6 Å). Conversely, outside domains 1A and 2A the structural change was significantly greater with an RMSD of 1.8 Å. Especially remarkable is an approximately 29° rotation of the 1B domain toward the ZBD upon nucleic acid binding. At the same time, the part of the nucleic acid substrate channel that is formed by domains 1A and 1B assumes an open conformation that is 2 Å wider than in the absence of the substrate. Nevertheless, the channel remains too narrow for entry of a duplex. This may suggest that unwinding is achieved by a structural element at the entrance of the substrate channel that destabilizes the duplex and makes one of the strands available for being pulled into the channel. In line with this model, the area around the entry site for the nucleic acid strand appeared to be heavily positively charged (Fig. 7) and may thus be utilized to bend the duplex during active unwinding, as seen for PcrA, or to guide the displaced strand. However, as the double-stranded part of the DNA could not be modeled, neither the presence nor the identity of the putative element that facilitates unwinding of double-stranded polynucleotides were established. Intriguingly, also surface regions in domain 1B and the ZBD that are not part of the substrate channel itself were substantially affected by DNA binding. Thus, it seems plausible that these two domains have a direct role in the presumably substrate-dependent binding of interaction partners.

In conclusion, the crystal structure of EAV nsp10 reinforces a common notion that nidovirus helicases may have evolved

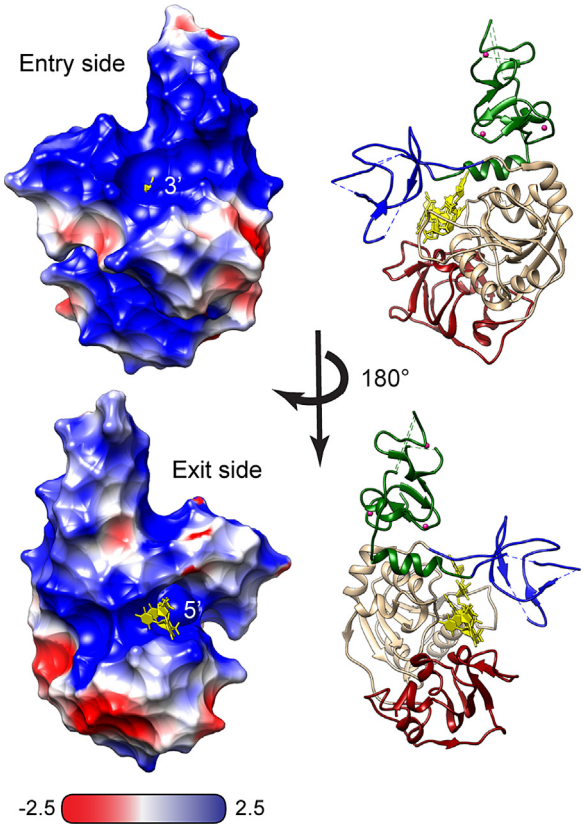

Fig. 7. Surface electrostatic potential of an EAV nsp10-DNA complex. Both entry and exit side of the protein's nucleic acid binding channel are predominantly positively charged, potentially providing binding surfaces for nucleic acid. Electrostatic potential mapped onto the molecular surface of 4N0O. Ribbon diagrams are colored as in Fig. 5. Red and blue colored regions denote negative and positive surface charges, respectively.

N- and/or C-terminal extensions in order to utilize the central helicase core enzymatic activities in many processes of the viral replication cycle (see Section 3.3. for functional implications). Of special interest is the presence of an N-terminal ZBD representing a novel complex zinc-binding fold and having structural similarity to the CH-domain of the cellular helicase Upf1 that is known to be involved in a number of RNA quality control pathways (Imamachi et al., 2012). This virus-host similarity is striking since it is observed despite a pronounced divergence of the ZBD among nidoviruses. Indeed, the size differences between the ZBDs of different nidovirus families are considerable, and just a dozen invariant residues mostly involved in zinc binding are shared by ZBDs. In line with these observations, replacement of EAV nsp10 residues 4 to 63 by the orthologous nsp10 ZBD sequence from PRRSV, another arterivirus, results in a total of 31 substitutions and six deletions and was not compatible with EAV viability (van Dinten et al., 2000). Thus, it may be possible that the interaction network between the ZBD and the helicase core is species-specific and may, especially in the large ZBDs of coronaviruses, impose a more complex regulation on the helicase core than is now apparent from the EAV nsp10 data. Moreover, it cannot be excluded that larger ZBDs may harbor additional structural elements that may further expand their functional repertoire.

3.3. Helicase function: a protein with diverse properties critically involved in several processes

Our understanding of the functions of helicase proteins in the nidovirus replication cycle has been and continues to be informed by functional studies using different techniques. Some of these studies, *e.g.* those dealing with the characterization of the genome, enzymatic activities and helicase structure, were already reviewed in the sections above. They will be mentioned below to the extent that is sufficient to connect them to other nidovirus studies, primarily employing reverse-genetics and molecular biology techniques, and also to functional paradigms in the helicase field.

3.3.1. Helicase and genome replication

Due to its genetic segregation with the RdRp, helicases of single-strand RNA viruses could be considered principally replicative helicases. As such, they might function in a manner reminiscent of better studied DNA helicases that participate in the replication of the double-stranded genomes of prokaryotes and eukaryotes. Obviously, this parallel is only valid if it also accounts for specifics of the replication and transcription of the single-stranded RNA genomes of nidoviruses. In this context, several helicase roles can be envisioned. First, the enzyme could support the polymerase by removing any obstacles the replication complex may encounter, for instance secondary structures in single-stranded templates, thereby increasing polymerase processivity (Kadare and Haenni, 1997). This model assumes proximity of or even interaction between the RdRp and helicase, which was shown for a number of helicases, for example SARS-CoV nsp13 and SF2 HCV NS3, to considerably stimulate their activity (Adedeji et al., 2012a; Cha and Alberts, 1989; Sladewski et al., 2011; Zhang et al., 2005). Still, since template-based nucleic acid synthesis proceeds in the 5′–3′ direction, and polymerases thus translocate with the opposite polarity along the template, only helicases with a 3′–5′ polarity will be able to stay associated with a replication complex of which the RdRp and helicase move along the same single strand (Fig. 8A). Thus, the 5′–3′ polarity of the helicases of nidoviruses and also alphaviruses (Bautista et al., 2002; Das et al., 2014; Ivanov et al., 2004; Seybert et al., 2000a,b; Tanner et al., 2003) seems to be incompatible with the conventional model of the active helicase associating with a polymerase using a single-stranded template, as became clear immediately when this polarity was first described (Seybert et al., 2000a). Alternatively, the RdRp alone may be capable of unwinding short stretches of secondary structure in single-stranded templates during RNA synthesis (Fig. 8B) while the helicase would separate the strands of dsRNA. In this model, the RdRp and helicase may not collide and could even cooperate as they would move in the same direction but along the complementary strands to exercise their respective activities (Fig. 8C). Since molecules resembling either blunt-ended replicative form (RF) or 3′-polyA-tailed replicative intermediate (RI), which are expected to be formed during replication and/or transcription (see below) by different mechanisms, did not support the activity of nidovirus helicases tested so far in *in vitro* experiments (Ivanov et al., 2004; Seybert et al., 2000a,b; Tanner et al., 2003), the model depicted in Fig. 8C depends on the involvement of other co-factors. For instance and obviously, cooperation of the helicase with other proteins that bind double-stranded RNA may facilitate its interaction with RF/RI as a step toward initiating unwinding once thermal fraying occurs.

To formally establish interactions with other (non-structural) proteins, two-hybrid screens of SARS-CoV proteins were conducted. These identified three possible interaction partners of nsp13: the accessory protein 3b encoded by an sg RNA, the RdRp nsp12, and a domain of the trans-membrane nsp3, which is the largest non-structural protein of coronaviruses and was also shown to bind to several other enzymes implicated in RNA replication, like the RdRp, the 3′–5′ exoribonuclease (ExoN) and N^7-methyltransferase (N-MT) (nsp14), and the 2′-O-methyltransferase (O-MT) (nsp16) (Imbert et al., 2008; Pan et al., 2008; von Brunn et al., 2007). Additionally, nsp13 was found to localize to presumably endoplasmic reticulum-derived membranous replication

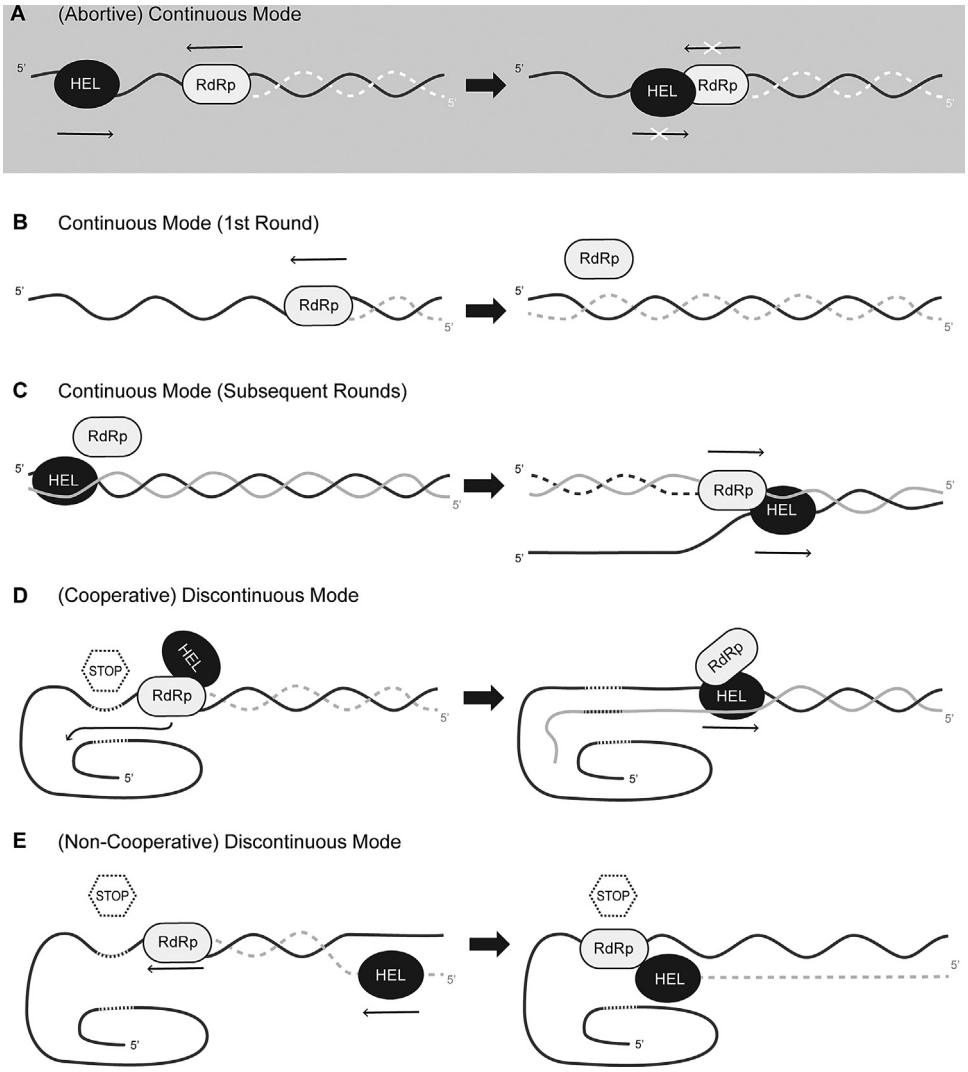

Fig. 8. Schematic representation of possible functions of the nidovirus helicase (HEL) in cooperation with the viral polymerase (RdRp) during genome replication and transcription. (A) Abortive replication and unwinding. Simultaneous RNA synthesis and unwinding of secondary structures of the template strand would lead to collision due to opposite polarities of HEL and RdRp with respect to a single-stranded template. (B) During the first round of continuous RNA synthesis on a single strand HEL may not be required. Note that this model assumes that the RdRp is able to remove secondary structures from the template strand. (C) Unwinding of double-stranded replication intermediates after the first round of RNA synthesis enables HEL and RdRp to traverse in the same direction along different strands: HEL along the positive strand (black), RdRp along the negative strand (gray). Note that nidovirus HEL is unable to initiate at blunt ends *in vitro* and thus presumably would require additional loading factors. (D) During discontinuous negative-strand RNA synthesis the RdRp may stall at a body TRS (dashed and stop symbol). Associated inactive HEL may subsequently facilitate switching to the leader TRS thus enabling addition of the anti-leader sequence without dissociation of RdRp and nascent strand. After completion of negative-strand synthesis, the RdRp becomes inactive. In order to increase HEL processivity, the RdRp stays associated with HEL that is traversing along the template strand (black) to separate the negative-sense subgenome-length RNA. Additional proteins required for circularization were omitted from the scheme for clarity. Inspired by (Enjuanes et al., 2006). (E) HEL may trail behind the synthesizing RdRp. Once RNA synthesis stalls at a body TRS, continued translocation along the nascent strand would lead to removal of this strand from the RdRp active site once HEL and RdRp collide. The 3′ end of the released nascent strand, carrying the body TRS complement, may subsequently base-pair with the leader TRS. Finally, the same or a second RdRp molecule may add the anti-leader sequence. Additional proteins required for circularization and potentially TRS base-pairing were omitted from the scheme for clarity.

structures in infected cells (Ivanov et al., 2004), which is very similar to the localization of most other non-structural proteins of related nidoviruses (Li et al., 2012; van der Meer et al., 1999). These findings indicate that nsp13 is, as expected, most likely part of the membrane-bound replication complex, an assumption further supported by findings from a complementation assay. Using EAV replicons, mutants deficient in nsp10 activity could not be complemented *in trans* by either simultaneous or exclusive expression of wild-type nsp10 from an IRES element inserted downstream of the replicase gene (van Dinten et al., 2000). The most likely explanation, besides technical reasons, is the apparently aberrant cytoplasmic localization of ectopically expressed nsp10. This suggests that nsp10 needs to be expressed in the context of the replicase polyprotein, which likely enables correct complex formation, in order to fulfill its role during virus replication. On the other hand, it cannot be excluded at present that nsp10-containing cleavage intermediates may have a separate function early in virus replication (van Dinten et al., 1996, 2000). Regardless which interpretation is true, both would require the co-expression of the RdRp and helicase proteins during infection, as was expected from the co-segregation of the respective genetic loci. In line with these considerations, a twofold stimulation of unwinding rate and almost doubling of the kinetic step size was detected upon addition of the cognate polymerase to the SARS-CoV helicase, while the ATPase rate remained unchanged (Adedeji et al., 2012a). Conversely, addition of the non-cognate RdRp of foot-and-mouth disease virus ($3D^{pol}$, *Picornaviridae* family) had no effect on any of the nsp13 parameters, indicating that a specific

interaction between RdRp and helicase is required to spur this enhanced activity.

3.3.2. Helicase and genome transcription

To rationalize the above observations, it may be informative to recapitulate the main facts on the unusual transcription mechanism of nidoviruses (reviewed in (Pasternak et al., 2006; Sawicki et al., 2007)). A common feature of this virus order is the generation of subgenome-size templates for sg mRNA synthesis, which is achieved by interruption of negative-strand RNA synthesis at specific RNA sequences. These signals, termed body TRSs, are located immediately upstream of the genes in the 3′-proximal part of the genome, whose expression depends on the production of sg mRNAs. In most but not all nidovirus groups (see below), following interruption of negative-strand synthesis, the nascent strand subsequently is translocated to the 5′ end of the genomic template where its 3′-terminal body TRS complement can base-pair with the so-called leader TRS. Next, negative-strand synthesis is resumed to add the complement of the genomic 5′ leader sequence. The subgenome-length negative strands then serve as templates for the synthesis of viral sg mRNAs, which thus carry the same 5′- and 3′-terminal sequences as the genome. Whereas all arteri-, corona-, and mesonivirus sg mRNAs appear to contain a leader that is identical to the genomic 5′ end, ronivirus sg mRNAs and all but the largest of the torovirus sg mRNAs lack such a common 5′ sequence, suggesting that their subgenome-length negative strands are functional templates for sg mRNA synthesis immediately after their release at a body TRS (Cowley et al., 2002; van Vliet et al., 2002; Zirkel et al., 2013). Thus, variations in the mechanism of subgenome-length negative strand RNA synthesis have evolved, which differ in their ability to resume negative-strand RNA synthesis after its interruption at a body TRS (Pasternak et al., 2006; Sawicki et al., 2007).

Although currently neither the protein complex(es) involved nor any detailed mechanisms for this process have been described, one of the explanations for the cooperativity between helicase and RdRp may be found in the context of this unique transcription mechanism. For example, both enzymes may be part of a complex that allows only one of the two proteins to be active at any given moment. It is conceivable that subgenome-length negative-strand RNA synthesis is started by a complex either lacking the helicase or including an enzymatically silent form (Fig. 8D). Once a body TRS is reached, the RNA sequence may stall the RdRp and during this pause association of the helicase may facilitate a template switch to the leader sequence. The latter may be positioned in close proximity to the original template strand if we assume that the genome is circularized *via* a protein bridge as seen for several other viruses (Sola et al., 2011). Implicitly, this model proposes that the nascent strand only dissociates from the RdRp when anti-leader sequence synthesis is completed. At this stage RdRp activity may be silenced and helicase activity may be triggered, leading to unwinding of the newly synthesized strand by the helicase's movement in the opposite direction (Fig. 8D). In consequence, partially double-stranded intermediates should arise under these conditions independent from helicase activity if helicase and RdRp cannot associate during the pause.

In an alternative model, the nidovirus helicase may trail behind the RdRp along the newly synthesized strand similar to the transcription termination factor rho (Ciampi, 2006) (Fig. 8E). Upon encountering a body TRS, the RdRp could stall till the lagging helicase reaches it. At this stage, the helicase would be in the position to pull the negative strand out of the RdRp active site and thereby potentially allowing polymerase dissociation. The nascent negative strand may then, possibly under guidance of additional proteins, base-pair with the leader TRS (again assuming genome circularization). Subsequently, the same or a second RdRp molecule may engage in extending the nascent negative strand with the anti-leader sequence. This model could also be modified to complete the synthesis of the negative strand using the original RdRp molecule assisted by an enzymatically inactive helicase molecule as depicted in Fig. 8D. The models in Fig. 8D and E could also be adapted to the utilization of sg mRNAs, rather than the genome, as template for the synthesis of complementary strands of other, smaller sg mRNAs, as described for coronaviruses (Sawicki et al., 2001; Wu and Brian, 2010). Once subgenome-length negative strands are produced, they may function as template for the respective sg mRNAs, according to the model in Fig. 8B and C. Thus, the above considerations envision differential requirements for helicase activity and helicase interaction with the RdRp in the continuous and discontinuous modes of RNA synthesis that operate during nidovirus replication and transcription. These processes may also recruit host helicase(s) (Wu et al., 2014), indicating that the proposed models may be modified as a result of future experimental probing.

To shed light on the validity of these hypotheses, it should be insightful to identify proteins or protein complexes that are modulated upon encountering a body TRS. Remarkably, the functional profile of a single-point mutant of EAV nsp10 showed that this protein may have properties compatible with the requirements of the template switching model (Fig. 8D). This mutant, with a replacement of residue S2429 of the replicase polyprotein (subsequently referred to as S59 of nsp10) by a proline, displayed a selective reduction of negative- and positive-sense subgenome-length RNA synthesis by ~100-fold, while genome synthesis and polyprotein processing remained unaltered (van Dinten et al., 1996; van Marle et al., 1999). Subsequent further probing of the same residue, which was originally thought to be located at the border between the ZBD and the helicase core, by replacing it with alanine, cysteine, glycine, histidine, leucine, or threonine led to no significant difference compared to wild-type nsp10 (van Dinten et al., 2000). Already at that time it was speculated that the special structural properties of proline in combination with a localization within a proposed hinge-region connecting the ZBD and the helicase core might be the cause of the mutant phenotype.

This hypothesis was recently verified and further refined on the basis of the EAV nsp10 crystal structure (Deng et al., 2014). It is now evident that this region of the protein appears to be an integral part of both the ZBD and a linker to the downstream region. S59, which notably is followed by another proline (P60), is located immediately downstream of the second zinc-binding module of the ZBD (Fig. 6) and contributes three main chain hydrogen bonds to the interactions with this module. These interactions are likely maintained in many mutants as long as the general backbone conformation of this loop is not significantly altered by, for instance, the introduction of a second proline (Deng et al., 2014). In agreement with this interpretation, also the introduction of consecutive glycines at position 59 and 60, which may lead to excessive flexibility, or inversion of the serine and proline resulted in phenotypes similar to that of the S59P mutant (van Dinten et al., 2000). Interestingly, when any of these three mutations was introduced into recombinant nsp10, the protein's activities in ATPase and helicase assays were almost indistinguishable from those of the wild-type protein, while the respective mutant viruses were severely crippled (Seybert et al., 2005; van Dinten et al., 2000). These observations suggested that the ZBD may have a vital function independent of the helicase activity *per se*, for example, in interacting with partners that facilitate the regulation or utilization of helicase functions. Remarkably, nsp10 is the third non-structural protein in arteriviruses, next to nsp1 (Nedialkova et al., 2010) and nsp11 (Posthuma et al., 2006), which was directly and specifically implicated in transcription. Given this specific effect on sg RNAs it seems plausible that interactions between nsp10 and other proteins play a role in discontinuous negative-strand synthesis. Therefore, it might be possible to

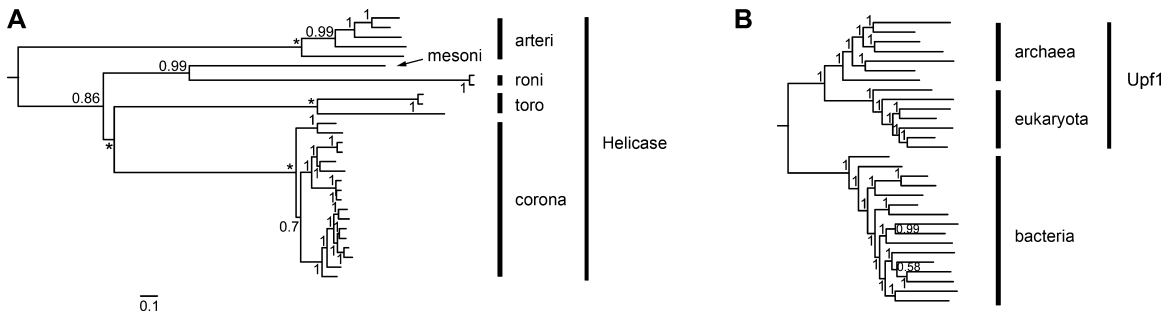

Fig. 9. Phylogeny of nidoviruses in comparison to the Tree of Life (ToL). Bayesian phylogenies of nidoviruses (A) and ToL (B) are drawn to a common scale of 0.1 amino acid substitutions per position. Major lineages are indicated by vertical bars and names; arteri: *Arteriviridae*, mesoni: *Mesoniviridae*, roni: *Roniviridae*, toro: *Torovirinae*, corona: *Coronavirinae*. Lineages encoding the nidovirus helicase or Upf1 are indicated. Rooting was according to either (A) domain-specific outgroups or (B) as described (Boussau et al., 2008). Posterior probability support values and fixed basal branch points (*) are indicated. The nidovirus and ToL alignments include, respectively, three enzymes and 56 single-gene protein families, 604 and 3336 columns, 2.95% and 2.8% gaps.
Adapted from Lauber et al. (2013).

rescue the EAV nsp10/S59P mutant virus by supplying negative-sense subgenome-length RNA templates separately.

3.3.3. Helicase and virion biogenesis

To gain insight into the function of the ZBD, its characterization was extended to point mutants of EAV nsp10 whose conserved zinc-binding histidine and cysteine residues were individually swapped. This approach was chosen with the goal of affecting but not impairing the protein's function by retaining the metal binding capacity, which was, however, not directly measured in the study. Despite this effort, RNA synthesis in general was still abolished in most mutants and, consequently, the respective mutations were lethal for the virus (Seybert et al., 2005; van Dinten et al., 2000). Where tested, this deficiency coincided with a loss or severe reduction (≥80%) of ATPase activity. The only mutants that were viable, although displaying delayed replication, a small-plaque phenotype, and lower progeny titers, were C25H and H44C, which *in vitro* had an up to 40% reduced ATPase activity and therefore also diminished helicase activity. Upon a more detailed investigation of their defects, total RNA synthesis of both mutants seemed to be severely reduced compared to the parental virus. Nevertheless, while C25H had apparently lower helicase activity than H44C, its progeny titer surprisingly was 100-fold higher. Furthermore, the 5-log decrease of H44C viability was not consistent with its relatively mild decrease in overall RNA synthesis. These results may indicate that EAV nsp10 has an additional function in processes downstream of RNA synthesis.

In line with the above findings, also a mutation that blocked the nsp10–nsp11 cleavage resulted in a lack of infectious progeny although genomic and sg RNAs were synthesized (van Dinten et al., 1999). Although this defect could also be explained by a late function of nsp11, it emphasizes the need for further investigation of the role of nsp10 in other steps than RNA synthesis. Such an additional function would not be unprecedented in the virus world as the helicase domain of the NS3 protein of several flaviviruses, but not its associated enzymatic activities, appear to be important for particle formation, potentially by providing interaction surfaces for other proteins including the core protein (Jones et al., 2011; Kummerer and Rice, 2002; Liu et al., 2002; Ma et al., 2008).

3.3.4. Helicase and translation

Next to its functions in RNA synthesis, biochemical data suggested a role for the helicase in translation through providing RNA 5′-triphosphatase activity implicated in mRNA capping (Ivanov et al., 2004; Ivanov and Ziebuhr, 2004). This activity was demonstrated in other RNA viruses with capped RNA, including alphavirus-like viruses (Balistreri et al., 2007; Benarroch et al., 2004; Karpe et al., 2011; Karpe and Lole, 2010b) and flaviviruses (Bartelma and Padmanabhan, 2002; Wengler and Wengler, 1991), which also encode other enzymatic activities involved in the production of capped RNAs. Based on this parallel, nidoviruses are expected to encode all components of the enzymatic capping machinery which has not been demonstrated yet for any nidovirus. For coronaviruses, a guanylyltransferase has not been identified (Subissi et al., 2014a), while two other major nidovirus groups lack also orthologs of the coronavirus N-MT (toroviruses) or N-MT and O-MT (arteriviruses) (Nga et al., 2011). Thus, the RNA 5′-triphosphatase activity of the helicase protein may be the only enzymatic activity of the capping machinery that is conserved across nidoviruses. Clearly, further research focusing on different lineages is required to ascertain the universal link between the conservation of the RNA 5′-triphosphatase activity of the helicase and cap formation.

3.3.5. Helicase and post-transcriptional quality control

In addition to being involved in replication, transcription, and translation, which has been proposed for helicases of other RNA virus families as well, nidovirus helicases may also engage in a unique post-transcriptional RNA surveillance and processing pathway. This hypothesis arose from the not totally surprising (see Fig. 2 in Gorbalenya and Koonin, 1993) but still provocative similarities to the highly conserved helicase Upf1 (Deng et al., 2014), which is universally employed by all eukaryotes (Fig. 9). As described above, those similarities involved not only the widely documented 5′–3′ polarity of unwinding and the lack of nucleic acid specificity, but also and uniquely the recently solved domain organization and fold. Most remarkably, Upf1 as well as nidovirus helicases carry a complex bipartite multi-nuclear zinc-binding domain at their N-terminus and an unstructured domain at their C-terminus, which both (probably) exert regulatory functions on the NTPase of these proteins (Cheng et al., 2007; Deng et al., 2014; Fiorini et al., 2013). The most conserved ZBD/CH and the helicase core domains of these two helicase lineages, nidovirus and Upf1, may be of monophyletic origin, while the evolutionary relationships of the least conserved domain are understandably untraceable. Given these parallels, it was speculated that, like Upf1 (Imamachi et al., 2012), nidovirus helicases could be involved in processes targeting aberrant viral transcripts, including the genome, for degradation (Deng et al., 2014), in order to prevent the synthesis of potentially harmful, truncated proteins. Alternatively, nidovirus helicases may be employed to interfere with Upf1-dependent pathways of the host by directly competing for interaction partners. In theory such interference may be a means to either protect viral RNAs from being recognized by and targeted to Upf1-dependent degradation pathways (Balistreri et al., 2014; Garcia et al., 2014) or to trigger the specific degradation of antiviral host mRNAs. The latter would mimic the type of

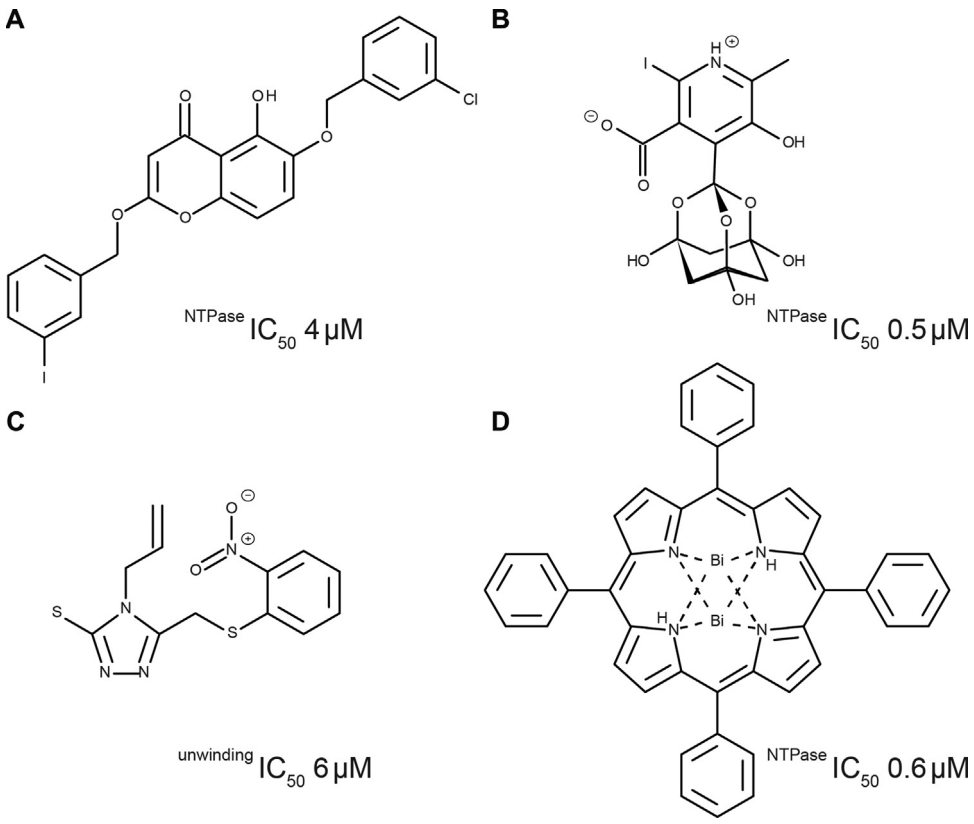

Fig. 10. Antiviral compounds with low cytotoxicity targeting SARS-CoV nsp13. Representative chemical structures of each inhibitor family. IC_{50} values refer to either NTPase or unwinding activity. (A) Chromones are inhibitors of NTPase activity. (B) Adamantine-derived bananines inhibit nucleic acid-stimulated NTPase activity non-competitively, while they do not affect unstimulated NTPase activity. (C) SSYA10-001 is a non-competitive inhibitor of unwinding but has no effect on NTPase activity. (D) Bismuth complexes act by releasing Bi^{3+}, which compete with Zn^{2+} for binding to the ZBD. Bi^{3+} are located above and below the plane of the porphyrin rings and are additionally coordinated by a solvent molecule.

regulation of mRNA abundance that is mediated by the host's non-sense mediated decay (NMD) machinery (Belew et al., 2014). Currently no data that link the nidovirus helicase with the stability of viral or cellular mRNAs are available. Similarly, RNA signals or proteins that could assist the helicase in the critical recognition of its wild-type or aberrant targets, particularly those of viral origin, remain uncharacterized. Thus, further experimental research is clearly needed to test the above hypotheses, which are not mutually exclusive.

The involvement of the helicase in NMD of abberant cognate RNAs might have been used to facilitate helicase gene fixation in the genome of an ancestral nidovirus. Given the restricted genome size variation in families of +RNA viruses (Gorbalenya et al., 2006), such facilitation could be essential since the helicase locus is larger than 1000 nucleotides and its acquisition must have increased genome size considerably. For nidoviruses, constraints on the genome size expansion were postulated to be linked to the fidelity of RNA replication and the division of labor between the three principal genome regions, ORF1a, ORF1b and the 3′-proximal ORFs (Lauber et al., 2013). These regions seem to have expanded largely in succession, with domain acquisition by ORF1b leading to the transition from small to large nidoviruses. Among the proteins acquired early on was the ExoN exoribonuclease, whose proofreading activity was likely critical for the fixation of this gene in the expanding ancestral genome. If it had not improved the fidelity of RNA synthesis, the expanded genome would have melted down due to its increased error load. The ExoN acquisition also relieved further genome expansions from fidelity constraints. Similar considerations were invoked to explain the fixation of the helicase gene in an ancestral nidovirus genome upon its transition from a helicase-free proto-ancestor with an astrovirus-like genome organization (Deng et al., 2014). It can be argued that with the helicase being involved in post-transcriptional mRNA quality control, progeny genomes that passed this quality control would carry fewer errors, an effect similar to, although likely with smaller impact than, that of ExoN proofreading during replication. In contrast, this effect would seem unlikely if the helicase were involved in the control of viral or cellular mRNA stability in the other two ways detailed above. Importantly, although the evolutionary considerations regarding the ancestral event favor one hypothesis over the other two, it remains to be established how this likely early specialization constrained further evolution of the nidovirus helicase. Consequently, all three hypotheses must be considered when studying contemporary nidoviruses.

4. Nidovirus helicases as drug targets

Despite intensified drug screening efforts since the 2003 SARS pandemic, clinically approved antivirals against nidoviruses are still lacking. Reflecting their importance during the viral replicative cycle, major drug targets are the chymotrypsin-like main protease (nsp5 in *Coronaviridae*), the RdRp, and also the helicase. As we have seen in the previous sections, helicase activity depends on several reactions and/or interactions: NTP binding, NTP hydrolysis, NDP and phosphate release, nucleic acid binding, translocation, duplex destabilization, protein co-factor binding, and signal transduction interconnecting any of these steps. Each of these may, at least in theory, be targeted to prevent unwinding. Consequently, the diversity of candidate drug scaffolds can be expected to be extensive, comprising NTP analogs and other small molecules, nucleic acid

competitors, as well as antibodies and aptamers (Kwong et al., 2005). The most accessible target in the helicase subunit probably is the NTP-binding site. However, given the similarity between viral and cellular NTPases and the vast number of proven and putative helicase enzymes in humans, many of the identified hits may possess significant cytotoxicity. To address this challenge, hit compounds are often first screened in unwinding assays and then counter-selected for NTPase inhibition. In this manner, molecules targeting less conserved regions and functions of the protein, for instance protein–protein interactions, which tend to be specific for each helicase, can be identified. Still, also this approach is hampered by the fact that helicase inhibition is often caused by intercalation into the nucleic acid substrate rather than binding to the enzyme itself (Shadrick et al., 2013).

Over the past years, four drug scaffolds with inhibitory effect on the SARS-CoV helicase and low cytotoxicity have been identified. Interestingly, the available biochemical data indicate that the modes of action of these inhibitors may be very different. First, chromone derivatives (Fig. 10A) and the adamantine-derived bananins (Fig. 10B) have a direct effect on the NTPase activity although they are not nucleotide analogs (Kim et al., 2011; Tanner et al., 2005). While chromones were not characterized in detail, bananins seemed to specifically inhibit nucleic acid-stimulated NTPase activity in a non-competitive fashion. Furthermore, these compounds did not inhibit the *E. coli* SF1 helicase DnaB, which suggests the presence of a non-conserved binding site on the surface of SARS-CoV nsp13. In agreement with this hypothesis, bananins exhibited good selectivity with an EC_{50} of <10 μM and CC_{50} of 390 μM. Whether this site may also be present in other nidovirus helicases has not been tested so far. Another non-competitive inhibitor was identified by Adedeji et al. (2012b, 2014). In contrast to the above compounds, it neither had an effect on the NTPase or nucleic acid-binding activities nor was it able to bind non-specifically to nucleic acids. Also this compound, designated SSYA10-001 (Fig. 10C) originating from the Maybridge HitFinder chemical library, did not inhibit the NS3 proteins of the two flaviviruses, HCV and Dengue virus. Moreover, it was efficacious against Middle East respiratory syndrome coronavirus (MERS-CoV), murine hepatitis virus (MHV), and SARS-CoV in cell culture, with EC_{50} values ranging from 7 to 25 μM while being non-toxic up to concentrations of 500 μM. Finally, bismuth complexes (Fig. 10D) proved to be effective against SARS-CoV in cell culture (EC_{50} 6 μM, CC_{50} 5 mM) (Yang et al., 2007a,b). As a mode of action it was proposed that bismuth ions can directly compete with zinc ions for their cysteine binding partners within the ZBD, thereby inhibiting NTPase and unwinding activities. It thus seems likely that these complexes may present broad-spectrum antiviral compounds against all nidoviruses.

5. Concluding remarks: a long and unwinding road to understanding nidovirus helicases

As detailed above, nidovirus helicases have been the subject of about a dozen, mostly biochemically oriented, studies involving a few mammalian viruses from the family *Arteriviridae* and subfamily *Coronavirinae*. These studies established the *in vitro* requirements for processivity and unidirectional 5′–3′ movement and their dependence on partially double-stranded DNA or RNA substrates and NTPase activity. The 5′–3′ directionality coupled with the requirement for a single-stranded overhang to initiate duplex unwinding is particularly restrictive with respect to RNA synthesis models, which can probably accommodate the helicase only upon postulating the involvement of additional and yet-to-be characterized co-factors. This and other properties of the nidovirus helicases listed above are shared with closely related helicases of viral and host origin. The overall similarity also includes the importance of a few highly conserved residues in the characteristic helicase motifs as well as the typical structural organization of the two core RecA-like domains, as revealed by the recent crystal structure of EAV nsp10.

The latter structure was also instrumental in establishing similarities between nidoviral and Upf1 helicases, creating a novel functional dimension that may be explored in future nidovirus research to assess the potential involvement of the helicase in post-transcriptional quality control. The helicase core domains of both the arterivirus nsp10 and Upf1 enzymes are covalently linked to apparently orthologous multinuclear Zn-binding domains, whose extensive interaction with other helicase and external domains may mediate signal transduction. Known as the ZBD (Zm) in nidoviruses, and distinguished by its exclusive presence in these viruses, this domain has been characterized extensively by site-directed mutagenesis and reverse genetics. From these studies it became clear that the arterivirus helicase is required for replication, transcription, and virion biogenesis. How the enzyme controls and possibly interconnects these processes are big unknowns that may not be resolved without major advancements in several fields, including the high-resolution visualization and *in vitro* reconstitution of the virus-specific intracellular factories that mediate major processes in the nidovirus replication cycle. These lines of inquiry are at the cutting-edge of the currently pursued research efforts (see *e.g.* Knoops et al., 2008; Subissi et al., 2014b). Their progress may be greatly stimulated by the availability of temperature-sensitive and other conditional mutants, whose parallel characterization by traditional genetics, *e.g.* complementation and recombination, may be equally insightful (Sawicki et al., 2005). Together, these studies are expected to uncover the temporal and spatial dynamics of the interactions between the helicase and its partners, which have remained totally obscure so far. Admittedly, the generation and characterization of such mutants is time-consuming and requires unique expertise. These issues must be urgently addressed if our understanding of nidovirus helicase functions is to approach the level that has already been achieved for cellular helicases involved in other complex RNA-based processes, *e.g.* transcription or splicing (reviewed in Cordin and Beggs, 2013; Eisen and Lucchesi, 1998).

To understand the specifics of helicase functions in the different phylogenetic lineages and firmly establish nidovirus-wide and lineage-specific features, their experimental characterization must be extended beyond the currently studied small number of viruses. These studies may also address questions inspired by comparative genomics, like it was done with the prior verification of the helicase and ZBD assignments. For instance, genomics tells us that the helicase is expressed downstream of the RdRp in nidoviruses, while it is the other way around in alpha-, flavi- and picorna-like viruses. This large-scale evolutionary difference may be linked to fundamental constraints, whose nature remains as unclear as 25 years ago when this difference was first established (Gorbalenya et al., 1989a;). More recently, we have learned that in a helicase-based phylogeny coronaviruses cluster with invertebrate nidoviruses rather than with mammalian toroviruses with whom they share many more characteristics and form the *Coronaviridae* family (Nga et al., 2011). That study also established the mosaic conservation of ORF1b domains, including methyltransferases, in the major phylogenetic lineages of nidoviruses, which questions the universal role of the helicase's RTPase activity in forming the 5′end RNA cap of nidoviruses. Resolving these apparent conflicts, and others that could emerge from the on-going genomic characterization of nidoviruses, is a challenge for future experimental research. If met, the integration of mechanistic and evolutionary insights may help in developing effective drugs targeting nidovirus helicases. It will also ensure that our understanding of the details

and relative importance of helicase characteristics is informed by natural selection rather than formed by our perception.

Acknowledgements

The authors thank Alexander Kravchenko, Dmitry Samborskiy, and Igor Sidorov for maintenance of Viralis and its database. This work was supported by the European Union's Seventh Framework program (FP7/2007-2013) through the EUVIRNA project (European Training Network on +RNA virus replication and antiviral drug development, Grant agreement n° 264286), by The Netherlands Organization for Scientific Research (NWO; TOP-GO grant 700.10.352), by the Collaborative Agreement on Bioinformatics between Leiden University Medical Center and Moscow State University (MoBiLe), and by the Leiden University Fund.

References

Adedeji, A.O., Marchand, B., te Velthuis, A.J., Snijder, E.J., Weiss, S., Eoff, R.L., Singh, K., Sarafianos, S.G., 2012a. Mechanism of nucleic acid unwinding by SARS-CoV helicase. PLoS ONE 7, e36521.

Adedeji, A.O., Singh, K., Calcaterra, N.E., DeDiego, M.L., Enjuanes, L., Weiss, S., Sarafianos, S.G., 2012b. Severe acute respiratory syndrome coronavirus replication inhibitor that interferes with the nucleic acid unwinding of the viral helicase. Antimicrob. Agents Chemother. 56, 4718–4728.

Adedeji, A.O., Singh, K., Sarafianos, S.G., 2012c. Structural and biochemical basis for the difference in the helicase activity of two different constructs of SARS-CoV helicase. Cell. Mol. Biol. 58, 114–121.

Adedeji, A.O., Singh, K., Kassim, A., Coleman, C.M., Elliott, R., Weiss, S.R., Frieman, M.B., Sarafianos, S.G., 2014. Evaluation of SSYA10-001 as a replication inhibitor of SARS, MHV and MERS coronaviruses. Antimicrob. Agents Chemother. 58, 4894–4898.

Ali, J.A., Maluf, N.K., Lohman, T.M., 1999. An oligomeric form of *E. coli* UvrD is required for optimal helicase activity. J. Mol. Biol. 293, 815–834.

Arai, N., Arai, K., Kornberg, A., 1981. Complexes of Rep protein with ATP and DNA as a basis for helicase action. J. Biol. Chem. 256, 5287–5293.

Balistreri, G., Caldentey, J., Kaariainen, L., Ahola, T., 2007. Enzymatic defects of the nsP2 proteins of Semliki Forest virus temperature-sensitive mutants. J. Virol. 81, 2849–2860.

Balistreri, G., Horvath, P., Schweingruber, C., Zund, D., McInerney, G., Merits, A., Muhlemann, O., Azzalin, C., Helenius, A., 2014. The host nonsense-mediated mRNA decay pathway restricts mammalian RNA virus replication. Cell Host Microbe 16, 403–411.

Bartelma, G., Padmanabhan, R., 2002. Expression, purification, and characterization of the RNA 5′-triphosphatase activity of dengue virus type 2 nonstructural protein 3. Virology 299, 122–132.

Bautista, E.M., Faaberg, K.S., Mickelson, D., McGruder, E.D., 2002. Functional properties of the predicted helicase of porcine reproductive and respiratory syndrome virus. Virology 298, 258–270.

Belew, A.T., Meskauskas, A., Musalgaonkar, S., Advani, V.M., Sulima, S.O., Kasprzak, W.K., Shapiro, B.A., Dinman, J.D., 2014. Ribosomal frameshifting in the CCR5 mRNA is regulated by miRNAs and the NMD pathway. Nature 512, 265–269.

Benarroch, D., Selisko, B., Locatelli, G.A., Maga, G., Romette, J.L., Canard, B., 2004. The RNA helicase, nucleotide 5′-triphosphatase, and RNA 5′-triphosphatase activities of Dengue virus protein NS3 are Mg^{2+}-dependent and require a functional Walker B motif in the helicase catalytic core. Virology 328, 208–218.

Bhattacharya, A., Czaplinski, K., Trifillis, P., He, F., Jacobson, A., Peltz, S.W., 2000. Characterization of the biochemical properties of the human Upf1 gene product that is involved in nonsense-mediated mRNA decay. RNA 6, 1226–1235.

Bird, L.E., Brannigan, J.A., Subramanya, H.S., Wigley, D.B., 1998. Characterisation of *Bacillus stearothermophilus* PcrA helicase: evidence against an active rolling mechanism. Nucleic Acids Res. 26, 2686–2693.

Boursnell, M.E., Brown, T.D., Foulds, I.J., et al., 1987. Completion of the sequence of the genome of the coronavirus avian infectious bronchitis virus. J.Gen.Virol. 68 (Pt 1), 57–77.

Boussau, B., Blanquart, S., Necsulea, A., Lartillot, N., Gouy, M., 2008. Parallel adaptations to high temperatures in the Archaean eon. Nature 456, 942–945.

Cha, T.A., Alberts, B.M., 1989. The bacteriophage T4 DNA replication fork: only DNA helicase is required for leading strand DNA synthesis by the DNA polymerase holoenzyme. J. Biol. Chem. 264, 12220–12225.

Chen, Y.Z., Zhuang, W., Prohofsky, E.W., 1992. Energy flow considerations and thermal fluctuational opening of DNA base pairs at a replicating fork: unwinding consistent with observed replication rates. J. Biomol. Struct. Dyn. 10, 415–427.

Chen, H.W., Ruan, B., Yu, M., Wang, J., Julin, D.A., 1997. The RecD subunit of the RecBCD enzyme from *Escherichia coli* is a single-stranded DNA-dependent ATPase. J. Biol. Chem. 272, 10072–10079.

Cheng, Z., Muhlrad, D., Lim, M.K., Parker, R., Song, H., 2007. Structural and functional insights into the human Upf1 helicase core. EMBO J. 26, 253–264.

Ciampi, M.S., 2006. Rho-dependent terminators and transcription termination. Microbiology 152, 2515–2528.

Cole, C., Barber, J.D., Barton, G.J., 2008. The Jpred 3 secondary structure prediction server. Nucleic Acids Res. 36, W197–W201.

Cordin, O., Beggs, J.D., 2013. RNA helicases in splicing. RNA Biol. 10, 83–95.

Cowley, J.A., Dimmock, C.M., Walker, P.J., 2002. Gill-associated nidovirus of *Penaeus monodon* prawns transcribes 3′-coterminal subgenomic mRNAs that do not possess 5′-leader sequences. J. Gen. Virol. 83, 927–935.

Crooks, G.E., Hon, G., Chandonia, J.M., Brenner, S.E., 2004. WebLogo: a sequence logo generator. Genome Res. 14, 1188–1190.

Czaplinski, K., Weng, Y., Hagan, K.W., Peltz, S.W., 1995. Purification and characterization of the Upf1 protein: a factor involved in translation and mRNA degradation. RNA 1, 610–623.

Das, P.K., Merits, A., Lulla, A., 2014. Functional cross-talk between distant domains of chikungunya virus non-structural protein 2 is decisive for its RNA-modulating activity. J. Biol. Chem. 289, 5635–5653.

Decroly, E., Ferron, F., Lescar, J., Canard, B., 2012. Conventional and unconventional mechanisms for capping viral mRNA. Nat. Rev. Microbiol. 10, 51–65.

de Groot, R.J., Cowley, J.A., Enjuanes, L., et al., 2012. Order Nidovirales. In: King, A.M.Q., Adams, M.J., Carstens, E.B., et, al. (Eds.), Virus taxonomy. Ninth Report of the International Committee on Taxonomy of Viruses. Elsevier Academic Press, Amsterdam.

Den Boon, J.A., Snijder, E.J., Chirnside, E.D., de Vries, A.A., Horzinek, M.C., Spaan, W.J., 1991. Equine arteritis virus is not a togavirus but belongs to the coronavirus like superfamily. J. Virol. 65, 2910–2920.

Deng, Z., Lehmann, K.C., Li, X., Feng, C., Wang, G., Zhang, Q., Qi, X., Yu, L., Zhang, X., Feng, W., Wu, W., Gong, P., Tao, Y., Posthuma, C.C., Snijder, E.J., Gorbalenya, A.E., Chen, Z., 2014. Structural basis for the regulatory function of a complex zinc-binding domain in a replicative arterivirus helicase resembling a nonsense-mediated mRNA decay helicase. Nucleic Acids Res. 42, 3464–3477.

Dillingham, M.S., Wigley, D.B., Webb, M.R., 2000. Demonstration of unidirectional single-stranded DNA translocation by PcrA helicase: measurement of step size and translocation speed. Biochemistry 39, 205–212.

Dillingham, M.S., Soultanas, P., Wiley, P., Webb, M.R., Wigley, D.B., 2001. Defining the roles of individual residues in the single-stranded DNA binding site of PcrA helicase. Proc. Natl. Acad. Sci. U. S. A. 98, 8381–8387.

Eisen, A., Lucchesi, J.C., 1998. Unraveling the role of helicases in transcription. Bioessays 20, 634–641.

Enjuanes, L., Almazan, F., Sola, I., Zuniga, S., 2006. Biochemical aspects of coronavirus replication and virus–host interaction. Annu. Rev. Microbiol. 60, 211–230.

Eoff, R.L., Raney, K.D., 2006. Intermediates revealed in the kinetic mechanism for DNA unwinding by a monomeric helicase. Nat. Struct. Mol. Biol. 13, 242–249.

Fairman-Williams, M.E., Guenther, U.P., Jankowsky, E., 2010. SF1 and SF2 helicases: family matters. Curr. Opin. Struct. Biol. 20, 313–324.

Fiorini, F., Boudvillain, M., Le, H.H., 2013. Tight intramolecular regulation of the human Upf1 helicase by its N- and C-terminal domains. Nucleic Acids Res. 41, 2404–2415.

Fischer, C.J., Maluf, N.K., Lohman, T.M., 2004. Mechanism of ATP-dependent translocation of *E. coli* UvrD monomers along single-stranded DNA. J. Mol. Biol. 344, 1287–1309.

Frick, D.N., Rypma, R.S., Lam, A.M., Frenz, C.M., 2004. Electrostatic analysis of the hepatitis C virus NS3 helicase reveals both active and allosteric site locations. Nucleic Acids Res. 32, 5519–5528.

Garcia, D., Garcia, S., Voinnet, O., 2014. Nonsense-mediated decay serves as a general viral restriction mechanism in plants. Cell Host Microbe 16, 391–402.

Gomez de Cedron, M., Ehsani, N., Mikkola, M.L., Garcia, J.A., Kaariainen, L., 1999. RNA helicase activity of Semliki Forest virus replicase protein NSP2. FEBS Lett. 448, 19–22.

Gorbalenya, A.E., Koonin, E.V., 1989. Viral proteins containing the purine NTP-binding sequence pattern. Nucleic Acids Res. 17, 8413–8440.

Gorbalenya, A.E., Koonin, E.V., 1993. Helicases: amino acid sequence comparisons and structure–function relationships. Curr. Opin. Struct. Biol. 3, 419–429.

Gorbalenya, A.E., Koonin, E.V., Donchenko, A.P., Blinov, V.M., 1988. A novel superfamily of nucleoside triphosphate-binding motif containing proteins which are probably involved in duplex unwinding in DNA and RNA replication and recombination. FEBS Lett. 235, 16–24.

Gorbalenya, A.E., Koonin, E.V., Donchenko, A.P., Blinov, V.M., 1989a. Coronavirus genome: prediction of putative functional domains in the non-structural polyprotein by comparative amino acid sequence analysis. Nucleic Acids Res. 17, 4847–4861.

Gorbalenya, A.E., Koonin, E.V., Donchenko, A.P., Blinov, V.M., 1989b. Two related superfamilies of putative helicases involved in replication, recombination, repair and expression of DNA and RNA genomes. Nucleic Acids Res. 17, 4713–4730.

Gorbalenya, A.E., Enjuanes, L., Ziebuhr, J., Snijder, E.J., 2006. Nidovirales: evolving the largest RNA virus genome. Virus Res. 117, 17–37.

Gorbalenya, A.E., Lieutaud, P., Harris, M.R., Coutard, B., Canard, B., Kleywegt, G.J., Kravchenko, A.A., Samborskiy, D.V., Sidorov, I.A., Leontovich, A.M., Jones, T.A., 2010. Practical application of bioinformatics by the multidisciplinary VIZIER consortium. Antiviral Res. 87, 95–110.

Gros, C., Wengler, G., 1996. Identification of an RNA-stimulated NTPase in the predicted helicase sequence of the Rubella virus nonstructural polyprotein. Virology 217, 367–372.

Hacker, K.J., Alberts, B.M., 1992. Overexpression, purification, sequence analysis, and characterization of the T4 bacteriophage dda DNA helicase. J. Biol. Chem. 267, 20674–20681.

Hickson, I.D., Arthur, H.M., Bramhill, D., Emmerson, P.T., 1983. The *E. coli* uvrD gene product is DNA helicase II. Mol. Gen. Genet. 190, 265–270.
Hodgman, T.C., 1988. A new superfamily of replicative proteins. Nature 333, 22–23.
Hoffmann, M., Eitner, K., von Grotthuss, M., Rychlewski, L., Banachowicz, E., Grabarkiewicz, T., Szkoda, T., Kolinski, A., 2006. Three dimensional model of severe acute respiratory syndrome coronavirus helicase ATPase catalytic domain and molecular design of severe acute respiratory syndrome coronavirus helicase inhibitors. J. Comput. Aided Mol. Des. 20, 305–319.
Imamachi, N., Tani, H., Akimitsu, N., 2012. Up-frameshift protein 1 (UPF1): multitalented entertainer in RNA decay. Drug Discov. Ther. 6, 55–61.
Imbert, I., Snijder, E.J., Dimitrova, M., Guillemot, J.C., Lecine, P., Canard, B., 2008. The SARS-Coronavirus PLnc domain of nsp3 as a replication/transcription scaffolding protein. Virus Res. 133, 136–148.
Ivanov, K.A., Ziebuhr, J., 2004. Human coronavirus 229E nonstructural protein 13: characterization of duplex-unwinding, nucleoside triphosphatase, and RNA 5′-triphosphatase activities. J. Virol. 78, 7833–7838.
Ivanov, K.A., Thiel, V., Dobbe, J.C., van der Meer, Y., Snijder, E.J., Ziebuhr, J., 2004. Multiple enzymatic activities associated with severe acute respiratory syndrome coronavirus helicase. J. Virol. 78, 5619–5632.
Jankowsky, E., Fairman, M.E., 2007. RNA helicases – one fold for many functions. Curr. Opin. Struct. Biol. 17, 316–324.
Jones, D.M., Atoom, A.M., Zhang, X., Kottilil, S., Russell, R.S., 2011. A genetic interaction between the core and NS3 proteins of hepatitis C virus is essential for production of infectious virus. J. Virol. 85, 12351–12361.
Jongeneel, C.V., Formosa, T., Alberts, B.M., 1984. Purification and characterization of the bacteriophage T4 dda protein: a DNA helicase that associates with the viral helix-destabilizing protein. J. Biol. Chem. 259, 12925–12932.
Kadare, G., Haenni, A.L., 1997. Virus-encoded RNA helicases. J. Virol. 71, 2583–2590.
Kadare, G., David, C., Haenni, A.L., 1996. ATPase, GTPase, and RNA binding activities associated with the 206-kDa protein of turnip yellow mosaic virus. J. Virol. 70, 8169–8174.
Karpe, Y.A., Lole, K.S., 2010a. NTPase and 5′ to 3′ RNA duplex-unwinding activities of the hepatitis E virus helicase domain. J. Virol. 84, 3595–3602.
Karpe, Y.A., Lole, K.S., 2010b. RNA 5′-triphosphatase activity of the hepatitis E virus helicase domain. J. Virol. 84, 9637–9641.
Karpe, Y.A., Aher, P.P., Lole, K.S., 2011. NTPase and 5′-RNA triphosphatase activities of Chikungunya virus nsP2 protein. PLoS ONE 6, e22336.
Kelley, L.A., Sternberg, M.J., 2009. Protein structure prediction on the Web: a case study using the Phyre server. Nat. Protoc. 4, 363–371.
Kim, J.L., Morgenstern, K.A., Griffith, J.P., et al., 1998. Hepatitis C virus NS3 RNA helicase domain with a bound oligonucleotide: the crystal structure provides insights into the mode of unwinding. Structure 6 (1), 89–100.
Kim, M.K., Yu, M.S., Park, H.R., Kim, K.B., Lee, C., Cho, S.Y., Kang, J., Yoon, H., Kim, D.E., Choo, H., Jeong, Y.J., Chong, Y., 2011. 2,6-Bis-arylmethyloxy-5-hydroxychromones with antiviral activity against both hepatitis C virus (HCV) and SARS-associated coronavirus (SCV). Eur. J. Med. Chem. 46, 5698–5704.
Knoops, K., Kikkert, M., Worm, S.H., Zevenhoven-Dobbe, J.C., van der Meer, Y., Koster, A.J., Mommaas, A.M., Snijder, E.J., 2008. SARS-coronavirus replication is supported by a reticulovesicular network of modified endoplasmic reticulum. PLoS Biol. 6, e226.
Koonin, E.V., 1991. Similarities in RNA helicases. Nature 352, 290.
Korolev, S., Hsieh, J., Gauss, G.H., Lohman, T.M., Waksman, G., 1997. Major domain swiveling revealed by the crystal structures of complexes of *E. coli* Rep helicase bound to single-stranded DNA and ADP. Cell 90, 635–647.
Kummerer, B.M., Rice, C.M., 2002. Mutations in the yellow fever virus nonstructural protein NS2A selectively block production of infectious particles. J. Virol. 76, 4773–4784.
Kwong, A.D., Rao, B.G., Jeang, K.T., 2005. Viral and cellular RNA helicases as antiviral targets. Nat. Rev. Drug Discov. 4, 845–853.
Lahaye, A., Stahl, H., Thines-Sempoux, D., Foury, F., 1991. PIF1: a DNA helicase in yeast mitochondria. EMBO J. 10, 997–1007.
Lahaye, A., Leterme, S., Foury, F., 1993. PIF1 DNA helicase from *Saccharomyces cerevisiae*: biochemical characterization of the enzyme. J. Biol. Chem. 268, 26155–26161.
Lai, M.M., Patton, C.D., Stohlman, S.A., 1982. Replication of mouse hepatitis virus: negative-stranded RNA and replicative form RNA are of genome length. J. Virol. 44, 487–492.
Lauber, C., Ziebuhr, J., Junglen, S., Drosten, C., Zirkel, F., Nga, P.T., Morita, K., Snijder, E.J., Gorbalenya, A.E., 2012. Mesoniviridae: a proposed new family in the order Nidovirales formed by a single species of mosquito-borne viruses. Arch. Virol. 157, 1623–1628.
Lauber, C., Goeman, J.J., Parquet, M.C., Nga, P.T., Snijder, E.J., Morita, K., Gorbalenya, A.E., 2013. The footprint of genome architecture in the largest genome expansion in RNA viruses. PLoS Pathog. 9, e1003500.
Lee, J.Y., Yang, W., 2006. UvrD helicase unwinds DNA one base pair at a time by a two-part power stroke. Cell 127, 1349–1360.
Lee, N.R., Kwon, H.M., Park, K., Oh, S., Jeong, Y.J., Kim, D.E., 2010. Cooperative translocation enhances the unwinding of duplex DNA by SARS coronavirus helicase nsP13. Nucleic Acids Res. 38, 7626–7636.
Levin, M.K., Wang, Y.H., Patel, S.S., 2004. The functional interaction of the hepatitis C virus helicase molecules is responsible for unwinding processivity. J. Biol. Chem. 279, 26005–26012.
Levin, M.K., Gurjar, M., Patel, S.S., 2005. A Brownian motor mechanism of translocation and strand separation by hepatitis C virus helicase. Nat. Struct. Mol. Biol. 12, 429–435.
Li, Y., Tas, A., Snijder, E.J., Fang, Y., 2012. Identification of porcine reproductive and respiratory syndrome virus ORF1a-encoded non-structural proteins in virus-infected cells. J. Gen. Virol. 93, 829–839.
Liu, W.J., Sedlak, P.L., Kondratieva, N., Khromykh, A.A., 2002. Complementation analysis of the flavivirus Kunjin NS3 and NS5 proteins defines the minimal regions essential for formation of a replication complex and shows a requirement of NS3 in cis for virus assembly. J. Virol. 76, 10766–10775.
Liu, B., Baskin, R.J., Kowalczykowski, S.C., 2013. DNA unwinding heterogeneity by RecBCD results from static molecules able to equilibrate. Nature 500, 482–485.
Lohman, T.M., Bjornson, K.P., 1996. Mechanisms of helicase-catalyzed DNA unwinding. Annu. Rev. Biochem. 65, 169–214.
Lucius, A.L., Vindigni, A., Gregorian, R., Ali, J.A., Taylor, A.F., Smith, G.R., Lohman, T.M., 2002. DNA unwinding step-size of *E. coli* RecBCD helicase determined from single turnover chemical quenched-flow kinetic studies. J. Mol. Biol. 324, 409–428.
Ma, Y., Yates, J., Liang, Y., Lemon, S.M., Yi, M., 2008. NS3 helicase domains involved in infectious intracellular hepatitis C virus particle assembly. J. Virol. 82, 7624–7639.
Maine, I.P., Kodadek, T., 1994. Inhibition of the DNA unwinding and ATP hydrolysis activities of the bacteriophage T4 DDA helicase by a sequence specific DNA–protein complex. Biochem. Biophys. Res. Commun. 198, 1070–1077.
Maluf, N.K., Lohman, T.M., 2003. Self-association equilibria of *Escherichia coli* UvrD helicase studied by analytical ultracentrifugation. J. Mol. Biol. 325, 889–912.
Maluf, N.K., Fischer, C.J., Lohman, T.M., 2003. A dimer of *Escherichia coli* UvrD is the active form of the helicase in vitro. J. Mol. Biol. 325, 913–935.
Manosas, M., Xi, X.G., Bensimon, D., Croquette, V., 2010. Active and passive mechanisms of helicases. Nucleic Acids Res. 38, 5518–5526.
Matson, S.W., 1986. *Escherichia coli* helicase II (urvD gene product) translocates unidirectionally in a 3′ to 5′ direction. J. Biol. Chem. 261, 10169–10175.
Matson, S.W., George, J.W., 1987. DNA helicase II of *Escherichia coli*: characterization of the single-stranded DNA-dependent NTPase and helicase activities. J. Biol. Chem. 262, 2066–2076.
Myong, S., Bruno, M.M., Pyle, A.M., Ha, T., 2007. Spring-loaded mechanism of DNA unwinding by hepatitis C virus NS3 helicase. Science 317, 513–516.
Nedialkova, D.D., Gorbalenya, A.E., Snijder, E.J., 2010. Arterivirus Nsp1 modulates the accumulation of minus-strand templates to control the relative abundance of viral mRNAs. PLoS Pathog. 6, e1000772.
Nga, P.T., Parquet, M.C., Lauber, C., Parida, M., Nabeshima, T., Yu, F., Thuy, N.T., Inoue, S., Ito, T., Okamoto, K., Ichinose, A., Snijder, E.J., Morita, K., Gorbalenya, A.E., 2011. Discovery of the first insect nidovirus, a missing evolutionary link in the emergence of the largest RNA virus genomes. PLoS Pathog. 7, e1002215.
Nishikiori, M., Sugiyama, S., Xiang, H., Niiyama, M., Ishibashi, K., Inoue, T., Ishikawa, M., Matsumura, H., Katoh, E., 2012. Crystal structure of the superfamily 1 helicase from Tomato mosaic virus. J. Virol. 86, 7565–7576.
Pan, J., Peng, X., Gao, Y., Li, Z., Lu, X., Chen, Y., Ishaq, M., Liu, D., DeDiego, M.L., Enjuanes, L., Guo, D., 2008. Genome-wide analysis of protein-protein interactions and involvement of viral proteins in SARS-CoV replication. PLoS ONE 3, e3299.
Pang, P.S., Jankowsky, E., Planet, P.J., Pyle, A.M., 2002. The hepatitis C viral NS3 protein is a processive DNA helicase with cofactor enhanced RNA unwinding. EMBO J. 21, 1168–1176.
Pasternak, A.O., Spaan, W.J., Snijder, E.J., 2006. Nidovirus transcription: how to make sense? J. Gen. Virol. 87, 1403–1421.
Posthuma, C.C., Nedialkova, D.D., Zevenhoven-Dobbe, J.C., Blokhuis, J.H., Gorbalenya, A.E., Snijder, E.J., 2006. Site-directed mutagenesis of the Nidovirus replicative endoribonuclease NendoU exerts pleiotropic effects on the arterivirus life cycle. J. Virol. 80, 1653–1661.
Preugschat, F., Averett, D.R., Clarke, B.E., Porter, D.J., 1996. A steady-state and pre-steady-state kinetic analysis of the NTPase activity associated with the hepatitis C virus NS3 helicase domain. J. Biol. Chem. 271, 24449–24457.
Pyle, A.M., 2008. Translocation and unwinding mechanisms of RNA and DNA helicases. Annu. Rev. Biophys. 37, 317–336.
Sagripanti, J.L., Zandomeni, R.O., Weinmann, R., 1986. The cap structure of simian hemorrhagic fever virion RNA. Virology 151, 146–150.
Saikrishnan, K., Griffiths, S.P., Cook, N., Court, R., Wigley, D.B., 2008. DNA binding to RecD: role of the 1B domain in SF1B helicase activity. EMBO J. 27, 2222–2229.
Saikrishnan, K., Powell, B., Cook, N.J., Webb, M.R., Wigley, D.B., 2009. Mechanistic basis of 5′–3′ translocation in SF1B helicases. Cell 137, 849–859.
Sawicki, D., Wang, T., Sawicki, S., 2001. The RNA structures engaged in replication and transcription of the A59 strain of mouse hepatitis virus. J. Gen Virol. 82, 385–396.
Sawicki, S.G., Sawicki, D.L., Younker, D., Meyer, Y., Thiel, V., Stokes, H., Siddell, S.G., 2005. Functional and genetic analysis of coronavirus replicase–transcriptase proteins. PLoS Pathog. 1, e39.
Sawicki, S.G., Sawicki, D.L., Siddell, S.G., 2007. A contemporary view of coronavirus transcription. J. Virol. 81, 20–29.
Seybert, A., Ziebuhr, J., 2001. Guanosine triphosphatase activity of the human coronavirus helicase. Adv. Exp. Med. Biol. 494, 255–260.
Seybert, A., Hegyi, A., Siddell, S.G., Ziebuhr, J., 2000a. The human coronavirus 229E superfamily 1 helicase has RNA and DNA duplex-unwinding activities with 5′ to 3′ polarity. RNA 6, 1056–1068.
Seybert, A., van Dinten, L.C., Snijder, E.J., Ziebuhr, J., 2000b. Biochemical characterization of the equine arteritis virus helicase suggests a close functional relationship between arterivirus and coronavirus helicases. J. Virol. 74, 9586–9593.

Seybert, A., Posthuma, C.C., van Dinten, L.C., Snijder, E.J., Gorbalenya, A.E., Ziebuhr, J., 2005. A complex zinc finger controls the enzymatic activities of nidovirus helicases. J. Virol. 79, 696–704.

Shadrick, W.R., Ndjomou, J., Kolli, R., Mukherjee, S., Hanson, A.M., Frick, D.N., 2013. Discovering new medicines targeting helicases: challenges and recent progress. J. Biomol. Screen. 18, 761–781.

Singleton, M.R., Wigley, D.B., 2002. Modularity and specialization in superfamily 1 and 2 helicases. J. Bacteriol. 184, 1819–1826.

Singleton, M.R., Scaife, S., Wigley, D.B., 2001. Structural analysis of DNA replication fork reversal by RecG. Cell 107, 79–89.

Singleton, M.R., Dillingham, M.S., Gaudier, M., Kowalczykowski, S.C., Wigley, D.B., 2004. Crystal structure of RecBCD enzyme reveals a machine for processing DNA breaks. Nature 432, 187–193.

Singleton, M.R., Dillingham, M.S., Wigley, D.B., 2007. Structure and mechanism of helicases and nucleic acid translocases. Annu. Rev. Biochem. 76, 23–50.

Sladewski, T.E., Hetrick, K.M., Foster, P.L., 2011. *Escherichia coli* Rep DNA helicase and error-prone DNA polymerase IV interact physically and functionally. Mol. Microbiol. 80, 524–541.

Sola, I., Mateos-Gomez, P.A., Almazan, F., Zuniga, S., Enjuanes, L., 2011. RNA–RNA and RNA–protein interactions in coronavirus replication and transcription. RNA Biol. 8, 237–248.

Stenglein, M.D., Jacobson, E.R., Wozniak, E.J., et al., 2014. Ball python nidovirus: a candidate etiologic agent for severe respiratory disease in *Python regius*. MBio 5 (5), e01484–e014814.

Subissi, L., Imbert, I., Ferron, F., Collet, A., Coutard, B., Decroly, E., Canard, B., 2014a. SARS-CoV ORF1b-encoded nonstructural proteins 12–16: replicative enzymes as antiviral targets. Antiviral Res. 101, 122–130.

Subissi, L., Posthuma, C.C., Collet, A., Zevenhoven-Dobbe, J.C., Gorbalenya, A.E., Decroly, E., Snijder, E.J., Canard, B., Imbert, I., 2014b. One severe acute respiratory syndrome coronavirus protein complex integrates processive RNA polymerase and exonuclease activities. Proc. Natl. Acad. Sci. U. S. A. 111, E3900–E3909.

Subramanya, H.S., Bird, L.E., Brannigan, J.A., Wigley, D.B., 1996. Crystal structure of a DExx box DNA helicase. Nature 384, 379–383.

Suzich, J.A., Tamura, J.K., Palmer-Hill, F., Warrener, P., Grakoui, A., Rice, C.M., Feinstone, S.M., Collett, M.S., 1993. Hepatitis C virus NS3 protein polynucleotide-stimulated nucleoside triphosphatase and comparison with the related pestivirus and flavivirus enzymes. J. Virol. 67, 6152–6158.

Tanner, J.A., Watt, R.M., Chai, Y.B., Lu, L.Y., Lin, M.C., Peiris, J.S., Poon, L.L., Kung, H.F., Huang, J.D., 2003. The severe acute respiratory syndrome (SARS) coronavirus NTPase/helicase belongs to a distinct class of 5′ to 3′ viral helicases. J. Biol. Chem. 278, 39578–39582.

Tanner, J.A., Zheng, B.J., Zhou, J., Watt, R.M., Jiang, J.Q., Wong, K.L., Lin, Y.P., Lu, L.Y., He, M.L., Kung, H.F., Kesel, A.J., Huang, J.D., 2005. The adamantane-derived bananins are potent inhibitors of the helicase activities and replication of SARS coronavirus. Chem. Biol. 12, 303–311.

Thiel, V., Ivanov, K.A., Putics, A., Hertzig, T., Schelle, B., Bayer, S., Weissbrich, B., Snijder, E.J., Rabenau, H., Doerr, H.W., Gorbalenya, A.E., Ziebuhr, J., 2003. Mechanisms and enzymes involved in SARS coronavirus genome expression. J. Gen. Virol. 84, 2305–2315.

Tijms, M.A., van der Meer, Y., Snijder, E.J., 2002. Nuclear localization of non-structural protein 1 and nucleocapsid protein of equine arteritis virus. J. Gen. Virol. 83, 795–800.

Tomko, E.J., Fischer, C.J., Niedziela-Majka, A., Lohman, T.M., 2007. A nonuniform stepping mechanism for *E. coli* UvrD monomer translocation along single-stranded DNA. Mol. Cell 26, 335–347.

Toseland, C.P., Martinez-Senac, M.M., Slatter, A.F., Webb, M.R., 2009. The ATPase cycle of PcrA helicase and its coupling to translocation on DNA. J. Mol. Biol. 392, 1020–1032.

van der Meer, Y., Snijder, E.J., Dobbe, J.C., Schleich, S., Denison, M.R., Spaan, W.J., Locker, J.K., 1999. Localization of mouse hepatitis virus nonstructural proteins and RNA synthesis indicates a role for late endosomes in viral replication. J. Virol. 73, 7641–7657.

van Dinten, L.C., Wassenaar, A.L., Gorbalenya, A.E., Spaan, W.J., Snijder, E.J., 1996. Processing of the equine arteritis virus replicase ORF1b protein: identification of cleavage products containing the putative viral polymerase and helicase domains. J. Virol. 70, 6625–6633.

van Dinten, L.C., Rensen, S., Gorbalenya, A.E., Snijder, E.J., 1999. Proteolytic processing of the open reading frame 1b-encoded part of arterivirus replicase is mediated by nsp4 serine protease and is essential for virus replication. J. Virol. 73, 2027–2037.

van Dinten, L.C., van Tol, H., Gorbalenya, A.E., Snijder, E.J., 2000. The predicted metal-binding region of the arterivirus helicase protein is involved in subgenomic mRNA synthesis, genome replication, and virion biogenesis. J. Virol. 74, 5213–5223.

van Marle, G., van Dinten, L.C., Spaan, W.J., Luytjes, W., Snijder, E.J., 1999. Characterization of an equine arteritis virus replicase mutant defective in subgenomic mRNA synthesis. J. Virol. 73, 5274–5281.

van Vliet, A.L., Smits, S.L., Rottier, P.J., de Groot, R.J., 2002. Discontinuous and non-discontinuous subgenomic RNA transcription in a nidovirus. EMBO J. 21, 6571–6580.

Velankar, S.S., Soultanas, P., Dillingham, M.S., Subramanya, H.S., Wigley, D.B., 1999. Crystal structures of complexes of PcrA DNA helicase with a DNA substrate indicate an inchworm mechanism. Cell 97, 75–84.

von Brunn, A., Teepe, C., Simpson, J.C., Pepperkok, R., Friedel, C.C., Zimmer, R., Roberts, R., Baric, R., Haas, J., 2007. Analysis of intraviral protein–protein interactions of the SARS coronavirus ORFeome. PLoS ONE 2, e459.

von Hippel, P.H., Delagoutte, E., 2001. A general model for nucleic acid helicases and their "coupling" within macromolecular machines. Cell 104, 177–190.

Walker, J.E., Saraste, M., Runswick, M.J., et al., 1982. Distantly related sequences in the alpha- and beta-subunits of ATP synthase, myosin, kinases and other ATP-requiring enzymes and a common nucleotide binding fold. EMBO J. 1 (8), 945–951.

Wang, Q., Han, Y., Qiu, Y., Zhang, S., Tang, F., Wang, Y., Zhang, J., Hu, Y., Zhou, X., 2012. Identification and characterization of RNA duplex unwinding and ATPase activities of an alphatetravirus superfamily 1 helicase. Virology 433, 440–448.

Wang, X., Lee, W.M., Watanabe, T., Schwartz, M., Janda, M., Ahlquist, P., 2005. Brome mosaic virus 1a nucleoside triphosphatase/helicase domain plays crucial roles in recruiting RNA replication templates. J. Virol. 79, 13747–13758.

Wengler, G., Wengler, G., 1991. The carboxy-terminal part of the NS 3 protein of the West Nile flavivirus can be isolated as a soluble protein after proteolytic cleavage and represents an RNA-stimulated NTPase. Virology 184, 707–715.

Wong, I., Lohman, T.M., 1992. Allosteric effects of nucleotide cofactors on *Escherichia coli* Rep helicase-DNA binding. Science 256, 350–355.

Wong, I., Moore, K.J., Bjornson, K.P., Hsieh, J., Lohman, T.M., 1996. ATPase activity of *Escherichia coli* Rep helicase is dramatically dependent on DNA ligation and protein oligomeric states. Biochemistry 35, 5726–5734.

Wu, H.Y., Brian, D.A., 2010. Subgenomic messenger RNA amplification in coronaviruses. Proc. Natl. Acad. Sci. U. S. A. 107, 12257–12262.

Wu, C.H., Chen, P.J., Yeh, S.H., 2014. Nucleocapsid phosphorylation and RNA helicase DDX1 recruitment enables coronavirus transition from discontinuous to continuous transcription. Cell Host Microbe 16, 462–472.

Xiang, H., Ishibashi, K., Nishikiori, M., Jaudal, M.C., Ishikawa, M., Katoh, E., 2012. Expression, purification, and functional characterization of a stable helicase domain from a tomato mosaic virus replication protein. Protein Expr. Purif. 81, 89–95.

Yang, N., Tanner, J.A., Wang, Z., Huang, J.D., Zheng, B.J., Zhu, N., Sun, H., 2007a. Inhibition of SARS coronavirus helicase by bismuth complexes. Chem. Commun. 42, 4413–4415.

Yang, N., Tanner, J.A., Zheng, B.J., Watt, R.M., He, M.L., Lu, L.Y., Jiang, J.Q., Shum, K.T., Lin, Y.P., Wong, K.L., Lin, M.C., Kung, H.F., Sun, H., Huang, J.D., 2007b. Bismuth complexes inhibit the SARS coronavirus. Angew. Chem. Int. Ed. Engl. 46, 6464–6468.

Yarranton, G.T., Gefter, M.L., 1979. Enzyme-catalyzed DNA unwinding: studies on *Escherichia coli* rep protein. Proc. Natl. Acad. Sci. U. S. A. 76, 1658–1662.

Zhang, C., Cai, Z., Kim, Y.C., Kumar, R., Yuan, F., Shi, P.Y., Kao, C., Luo, G., 2005. Stimulation of hepatitis C virus (HCV) nonstructural protein 3 (NS3) helicase activity by the NS3 protease domain and by HCV RNA-dependent RNA polymerase. J. Virol. 79, 8687–8697.

Zirkel, F., Roth, H., Kurth, A., Drosten, C., Ziebuhr, J., Junglen, S., 2013. Identification and characterization of genetically divergent members of the newly established family Mesoniviridae. J. Virol. 87, 6346–6358.